OXFORD UNIVERSITY PRESS | Cerebral Cortex

Pain-evoked reorganization in functional brain networks

Journal:	*Cerebral Cortex*
Manuscript ID	CerCor-2019-00120.R1
Manuscript Type:	Original Article
Date Submitted by the Author:	n/a
Complete List of Authors:	Zheng, Weihao; Zhejiang University, College of Biomedical Engineering and Instrument Science Woo, Choong-Wan; Sungkyunkwan University, Department of Biomedical Engineering Yao, Zhijun; Lanzhou University, School of Information Science and Engineering Goldstein, Pavel; University of Colorado Boulder, Department of Psychology and Neuroscience Atlas, Lauren; NIH, NCCAM Roy, Mathieu; Concordia University, Psychology Schmidt, Liane; INSERM, CR-ICM U975 Krishnan, Anjali ; Brooklyn College, Department of Psychology Jepma, Marieke ; Universiteit van Amsterdam, Department of Psychology Hu, Bin; Lanzhou University, School of Information Science and Engineering Wager, Tor; University of Colorado, Boulder, Psychology and Neuroscience
Keywords:	pain, functional network, reorganization, inter-system connectivity, hub disruption

Pain-evoked reorganization in functional brain networks

Weihao Zheng[1,2], Choong-Wan Woo[3,4], Zhijun Yao[1], Pavel Goldstein[5,6,7], Lauren Y. Atlas[8,9], Mathieu Roy[10], Liane Schmidt[11], Anjali Krishnan[12], Marieke Jepma[13], Bin Hu[1,*], Tor D. Wager[5,6,*]

[1] School of Information Science and Engineering, Lanzhou University, Lanzhou, 730000, P. R. China.

[2] College of Biomedical Engineering and Instrument Science, Zhejiang University, Hangzhou, 310027, P. R. China.

[3] Center for Neuroscience Imaging Research, Institute for Basic Science, Suwon 16419, Republic of Korea.

[4] Department of Biomedical Engineering, Sungkyunkwan University, Suwon 16419, Republic of Korea.

[5] Department of Psychology and Neuroscience, University of Colorado, Boulder, Colorado 80309, USA.

[6] Institute of Cognitive Science, University of Colorado, Boulder, CO 80309, USA.

[7] The School of Public Health, University of Haifa, Israel.

[8] National Center for Complementary and Integrative Health, National Institutes of Health, Bethesda, Maryland 20892, USA.

[9] National Institute on Drug Abuse, National Institutes of Health, Baltimore, Maryland 21224, USA.

[10] Department of Psychology, McGill University, Montréal, Quebec H3A 0G4, Canada.

[11] Affective Neuroscience (SAN) team, Institut du Cerveau et de la Moelle épinière (ICM), INSERM UMR 1127, CNRS UMR 7225, Sorbonne Université, 75013 Paris, France.

[12] Department of Psychology, Brooklyn College of the City University of New York, Brooklyn, New York 11210, USA.

[13] Department of Psychology, University of Amsterdam, Amsterdam, The Netherlands.

*Corresponding author:

Tor D. Wager

Email: tor.wager@colorado.edu

Bin Hu

Email: bh@lzu.edu.cn

Abstract

Recent studies indicate that a significant reorganization of cerebral networks may occur in patients with chronic pain, but how immediate pain experience influences the organization of large-scale functional networks is not yet well characterized. To investigate this question, we used functional magnetic resonance imaging in 106 participants experiencing both noxious and innocuous heat. Painful stimulation caused network-level reorganization of cerebral connectivity that differed substantially from organization during innocuous stimulation and standard resting-state networks. Noxious stimuli increased somatosensory network connectivity with (a) fronto-parietal networks involved in context representation, (b) 'ventral attention network' regions involved in motivated action selection, and (c) basal ganglia and brainstem regions. This resulted in reduced 'small-worldness', modularity (fewer networks), and global network efficiency, and in the emergence of an integrated 'pain supersystem' (PS) whose activity predicted individual differences in pain sensitivity across 5 participant cohorts. Network hubs were reorganized ('hub disruption') so that more hubs were localized in PS, and there was a shift from 'connector' hubs linking disparate networks to 'provincial' hubs connecting regions within PS. Our findings suggest that pain reorganizes the network structure of large-scale brain systems. These changes may prioritize responses to painful events and provide nociceptive systems privileged access to central control of cognition and action during pain.

Key words: immediate pain, functional network, reorganization, inter-system

connectivity, hub disruption

Introduction

Pain is a conscious experience defined as "an unpleasant sensory and emotional experience associated with actual or potential tissue damage, or described in terms of such damage" (https://www.iasp-pain.org). Noxious stimuli engage multiple systems distributed across the brain, including the insula, anterior cingulate cortex (ACC), amygdala (sometimes grouped under the rubric of 'salience network' or 'ventral attention network'), and somatosensory areas S1, S2, and dorsal posterior insula (part of the 'somatomotor network'), thalamus, and brainstem. The involvement of multiple functional systems suggests cooperation and integration in processing pain-related information, which may provide a substrate for generating the conscious experience of pain and prioritize access to action-planning systems (Bornhövd K et al. 2002; Apkarian AV et al. 2005; Tracey I and PW Mantyh 2007; Bastuji H et al. 2008; Boly M et al. 2008). Advances in functional brain imaging have allowed researchers to characterize patterns of functional activation and deactivation to painful stimuli across different types of evoked pain (Davis KD et al. 1997; Kwan CL et al. 2000; Bornhövd K *et al.* 2002; Wager TD et al. 2013; Favilla S et al. 2014; Krishnan A et al. 2016), predict pain intensity from patterns of brain activity (Wager TD *et al.* 2013; Atlas LY et al. 2014; Favilla S *et al.* 2014; Wiech K 2016; Lindquist MA et al. 2017), and identify brain mediators of pain (Atlas LY et al. 2010; Atlas LY *et al.* 2014; Woo C-W et al. 2015). Though important, these findings chiefly concern patterns of brain activity, and do not address the issue of how nociception and pain alter brain connectivity and modularity in functional brain networks.

The important issue of pain-related alterations in brain connectivity and network structure has recently been investigated in a series of important studies that have identified alterations in brain connectivity in both evoked experimental and chronic pain (Zaki J et al. 2007; Napadow V et al. 2010; Farmer MA et al. 2012; Jensen KB et al. 2012; Kong J et al. 2013; Kucyi A et al. 2014; Martucci KT et al. 2014; Kucyi A and KD Davis 2015; Hemington KS et al. 2016; Kutch JJ et al. 2017). For example, chronic pain is associated with abnormalities in functional connectivity (FC), e.g., increased FC between medial prefrontal cortex (mPFC) and regions that receive nociceptive affererents, including ACC and insula (Cauda F et al. 2009; Napadow V *et al*. 2010; Baliki MN et al. 2014; Kucyi A and KD Davis 2015). At the network level, chronic pain is associated with reduced task-related deactivation in the 'default mode network' (DMN, which includes mPFC) (Baliki MN et al. 2008; Baliki MN et al. 2011); reduced positive correlations among default-mode regions (Kornelsen J et al. 2013); reduced negative correlations between default-mode and other brain networks (Baliki MN *et al*. 2011), particularly the 'salience network' (SN; which contains the anterior insula) (Hemington KS *et al*. 2016); and increased correlations between the anterior and posterior insula with 'default mode'- and 'ventral attention'-related areas (Napadow V *et al*. 2010; Tagliazucchi E et al. 2010; Loggia ML et al. 2013).

Some studies have begun to analyze connectivity patterns in pain-related networks from the vantage point of network topology, using concepts from graph theory (Sporns O and JD Zwi 2004; Bullmore E and O Sporns 2009). Graph-theoretic analysis provides rich quantitative measures (Rubinov M and O Sporns 2010) that efficiently describe the segregation and integration of complex brain networks. Graph theoretic metrics serve as high-level topological features that can characterize complex alterations in neurodegenerative, neurological, and psychiatric disorders (Bullmore E and O Sporns 2009; van den Heuvel MP and O Sporns 2013; Fornito A et al. 2015; Yao Z et al. 2015; Sha Z et al. 2017; Zheng W et al. 2018). Pain studies have begun to identify altered network organization in chronic pain patients compared with normative samples (Mano H and B Seymour 2015; Mansour A et al. 2016; Mano H et al. 2018). For example, Mano et al. found evidence for several global network changes in chronic low back pain patients, including hub disruption (reorganization of regions that are highly connected), reduced mean clustering coefficient (a measure of whether regions are tightly inter-connected into functional modules), and reduced betweenness-centrality (incidence of 'connector nodes' that connect multiple networks). These changes were replicated across three separate patient samples (Mano H *et al*. 2018). Together, previous pain-related connectivity studies point to increased cross-talk among networks and reduced functional specialization in chronic pain, and particularly greater connectivity between the DMN and SN, which are usually anti-correlated (e.g., increased DMN connectivity with putatively pain-related regions in the insula).

Other studies have shown that resting-state functional connectivity predicts later symptom improvements. For example, increased connectivity among predominantly left fronto-parietal network regions has been reported to predict symptom improvements 3 months later in patients with urologic chronic pelvic pain (Kutch JJ *et al*. 2017). Increased connectivity between lateral prefrontal cortex and other regions (Tétreault P et al. 2016), and between mPFC and insula (Hashmi JA et al. 2012), has been found to predict the magnitude of subsequent placebo responses in chronic back pain patients.

In this paper, we attempted to address two inter-related issues not addressed in previous studies. First, the vast majority of connectivity studies have identified changes related to chronic pain, and to our knowledge there has been no systematic characterization of network topology in evoked experimental pain. Understanding the network topology of evoked pain would provide an important basis for comparing experimental and chronic pain. Second, previous studies of chronic pain have not separated connectivity related to pain experience itself from connectivity changes related to the *kinds of individuals* who experience pain. Pain patients differ from controls in many ways, including medication status, depression and anxiety, exercise and body weight, and socioeconomic status, among other variables. Thus, it is desirable to identify connectivity changes directly associated with nociception and pain experience (e.g., (Seminowicz DA and KD Davis 2007; Zaki J *et al*. 2007)), which may be compared with the more complex set of changes associated with individuals with chronic pain conditions.

We analyzed functional Magnetic Resonance Imaging (fMRI) data from 5 independent studies, with a total of 106 participants, to construct group-level functional networks for noxious (painfully hot) and innocuous (non-painful warmth) thermal stimuli, and characterize the differences between them. Rather than focusing on time series connectivity, we estimated functional connectivity matrices and network topology measures based on *inter-individual differences* (He Y et al. 2007; Wager TD et al. 2007; He Y et al. 2008; Evans AC 2013; Palaniyappan L et al. 2015; Yao Z *et al*. 2015). This (a) constrains connectivity estimates to brain responses to painful (or non-painful) stimulation, and (b) estimates networks such that 'connected' regions are co-activated in the same individuals, making network estimates more relevant for individual differences in pain sensitivity. Other benefits of estimating connectivity in stimulus-evoked responses averaged over trials is that it enhances the signal-to-noise ratio (SNR) for pain-related signals, reduces susceptibility to intrinsic neural dynamics and time series artifacts (Simony E et al. 2016), and reduces extraneous sources of inter-individual variability relative to resting-state studies (Geerligs L et al. 2015; Finn ES et al. 2017). Participants were selected to have matched numbers of noxious and innocuous thermal stimuli, to allow comparison of activity and individual differences between the two conditions. We then calculated graph-theoretic measures, including small-world-ness, modules and hub nodes, and connectivity patterns, to examine stimulus intensity-dependent and pain-dependent alterations in network organization. Overall, the results provided a coherent picture of reduced network diversity and complexity (across multiple graph-theoretic measures) during pain, paralleled by increased integration in particular cortical and subcortical systems.

Materials and Methods

Participants

For network analysis, we used fMRI data from 119 healthy participants (before exclusion criterion were applied) from 5 published studies (Atlas LY *et al.* 2010; Atlas LY et al. 2012; Atlas LY *et al.* 2014; Woo C-W *et al.* 2015; Lindquist MA *et al.* 2017). All studies were approved by the institutional review board of Columbia University and the University of Colorado Boulder. Participants were recruited from New York City and Boulder/Denver Metro Areas, and all participants provided written informed consent. Participants with psychiatric, physiological or pain disorders, neurological conditions, and MRI contraindications were excluded prior to enrollment. Preliminary eligibility of participants was determined through an online questionnaire, a pain safety screening form, and a functional Magnetic Resonance Imaging (fMRI) safety screening form. Descriptive information about age, gender, and other features of each study are provided in Table 1. In all studies, participants received a series of contact-heat stimulus using a TSA-II Neurosensory Analyzer (Medoc Ltd., Chapel Hill, NC) with a 16 mm Peltier thermode endplate (Study 7:32 mm), and rated the magnitude of pain they felt on a visual analog scale after stimulus offset. The number of trials, stimulation sites, rating scales, intensities and durations of stimulus, and the specific psychological manipulation each study comprised varied across studies as shown in Table 1 (also see Table S1 for details about the fMRI acquisition parameters). Notably, the psychological and physical manipulations that influenced pain (except for stimulus intensity) were irrelevant for our analyses, as our focus was on investigating the difference between noxious and innocuous stimuli in functional network organization, and all psychological manipulations were balanced across (orthogonal to) noxious and innocuous conditions.

Image preprocessing

Functional images were preprocessed using SPM software (http://www.fil.ion.ucl.ac.uk/spm/). Our goal was not to maintain perfect homogeneity in analyses across studies, but rather to establish broad generalizability across a range of studies with standard, but different, state-of-the-art methods. This has disadvantages in spatial precision (though we focus on pre-defined parcels, which mitigates this drawback), but has advantages in (a) establishing generalizability (e.g., (Kragel PA et al. 2018; Mano H *et al.* 2018; Zunhammer M et al. 2018)) and (b) maintaining consistency with published and quality-checked final analyses for each study. However, the normalization template and general linear model framework used were identical for all studies.

Briefly, structural T1-weighted images were co-registered to the average functional image for each subject with the mutual information based co-registration method in SPM, and were then normalized to Montreal Neurological Institute (MNI) space (avg152T1.nii). Functional images were corrected for slice-acquisition-timing and motion; warped to MNI space by applying motion parameters estimated from co-registered, high resolution structural images; interpolated to $2 \times 2 \times 2$ mm^3 voxels; and smoothed with an 8 mm FWHM Gaussian kernel.

Prior to processing, global outlier time points were identified by calculating the mean and standard deviation of intensity across voxels for each image. Mahalanobis distances were computed for the matrix of slice-wise mean and standard deviation values (concatenated) by functional volumes, and values with significant χ^2 value after multiple comparison correction (Bonferroni) were considered outliers. The outputs of this procedure were later included as nuisance covariates in the first level models. The number of removed volumes in each study can be found in referenced publications, but averages around 1% of functional volumes (Atlas LY *et al.* 2010; Atlas LY *et al.* 2012; Atlas LY *et al.* 2014; Woo C-W *et al.* 2015; Lindquist MA *et al.* 2017).

Single trial analyses

For studies except Study 3, magnitudes of single trial responses were quantified by constructing a GLM design matrix with separate regressors for each trial. Boxcar regressors, convolved with the canonical hemodynamic response function (HRF), were constructed to model cue, pain, and rating periods in each study. One regressor was included for each trial, as well as several types of nuisance covariates (images with high artifact/outlier scores as defined above, head movement parameter estimates). Because trial estimates could be strongly affected by artifacts occurring during acquisition (e.g. sudden motion), trial-by-trial variance inflation factors (VIF, a measure of design-induced uncertainty due, in this case, to collinearity with nuisance regressors) were calculated, and any trials with VIFs that exceeded 2.5 were excluded. For Study 1, trials that exceeded three standard deviations above the mean were excluded, and a principal components-based denoising approach during preprocessing to minimize artifacts was employed. This step generated single trial estimates that reflected the amplitude of the fitted HRF on each trial and referred to the magnitude of anticipatory and pain-period activity for each trial in each voxel.

For Study 3, single trial analyses were based on fitting a set of three basis functions, rather than on the canonical HRF. This flexible strategy allowed the shape of the modeled HRF to vary across trials and voxels. This procedure differed from other studies because it maintained consistency with the procedures used in the original publication (Atlas LY *et al.* 2010), and provided an opportunity to examine predictive performance using a flexible basis set. The pain period basis set consisted of three curves shifted in time and was customized for thermal pain responses based on previous studies (Lindquist MA et al. 2009; Atlas LY *et al.* 2010). To estimate cue-evoked responses, the pain anticipation period was modeled using a boxcar epoch convolved with a canonical HRF. This epoch was truncated at 8 sec to ensure that fitted anticipatory responses were not affected by noxious stimulus-evoked activity. As with the other studies, nuisance covariates and excluded trials with VIFs > 2.5 were included. Trials that were global outliers (those that exceeded 3 SDs above the mean) were also excluded. The fitted basis functions from the flexible single trial approach were reconstructed to compute the area under the curve (AUC) for each trial and in each voxel. These trial-by-trial AUC values were used as estimates of trial-level anticipatory or pain-period activity.

Categorization criteria of non-painful and painful stimulus

Previous studies have shown that the threshold for specific nociceptors is around 45 °C (LaMotte RH and JN Campbell 1978), and have identified human pain thresholds in the range of 45 - 46 °C (Price DD et al. 1989). Here, we used 45.3 °C as a threshold for dividing thermal stimulation into innocuous (stimulation intensity < 45.3 °C) and noxious (stimulation intensity > 45.3 °C) conditions. Participants with both of the two conditions were included. We excluded stimulation level of 49.3 °C in Study 2, as it included only four trials per participant. We also excluded subjects with missing heat ratings and trials delivered during drug administration and active placebo conditions. Finally, as our goal was to compare noxious and innocuous conditions across the same set of participants, for datasets with multiple stimulus intensities within the noxious or innocuous range, we randomly selected one stimulus level for analysis. A total of 106 participants remained in the final analysis. Detailed information regarding pain ratings and stimulation intensity of the included participants are shown in Figure S1. Painfully hot stimuli caused significant increases in intensity ratings relative to non-painful warmth and were in the clearly noxious stimulus range (46-49 °C), whereas warm stimuli were below the threshold for specific nociceptors.

Functional network construction

Figure 1 provides a flowchart of network construction. The single-trial images were generated by constructing a GLM over the entire time-course of the study for a given person, with one regressor per trial. The trial-level regressors modeled activity during each 10 sec stimulation epoch, which were convolved with the HRF. To reduce differences in image scaling across studies, we rescaled the activity of all included trials for the selected stimulus intensity study-wise, by the study's global average median absolute deviation (MAD). Then, trial-level maps were averaged at the same stimulation intensity within each subject to yield one pain-associated and one no-pain-associated image for each participant. Average activity was calculated for each of 274 brain parcels as defined in a recent atlas (the 'Brainnetome' atlas)(Fan L et al. 2016) with 210 cortical, 36 subcortical and 28 cerebellar regions spanning the brain (K = 274 in total). These averages were concatenated into a 274 × N matrix, where N is the number of subjects (i.e., 106). We then calculated a 274 x 274 matrix of Pearson correlations among regions (37,401 total connections). Prior to connectivity estimation, linear regression was applied within each study to remove the effects of white matter (WM), cerebral spinal fluid (CSF), and global grey matter (GM) signals, which were also rescaled and averaged across trials, from the regional activity estimates (i.e., the subjects × regions matrix for each of high-pain and low-pain conditions). Because the individual differences level is the level of primary interest here, regression at this level provides results that most closely related to the variables of interest. This is in addition to covariates included in the first-level models for head movement, spikes, and artifacts detected as outliers in global signal and root mean square successive deviations (dvars). We chose to regress out GM because previous studies have suggested that the removal of global GM signal may have little influence on community structure but can increase the signal to noise in task-related graph theoretic measures (Herrera LC et al. 2017). Graph metrics should thus be interpreted as inter-regional covariation around the whole-brain mean.

Module detection

The optimal division of module structure is the non-overlapping communities with maximization of intra-module edges and minimization of inter-module edges. Both negative connections and positive connections with weights near zero were excluded, because these links may represent spurious functional connections (Power JD et al. 2010; Rubinov M and O Sporns 2010). False discovery rate (FDR) correction with $q = 0.05$ was performed to remove the non-significant positive links by setting weights of links with p values above the threshold to 0 (Chen ZJ et al. 2008), and the resulting networks were used for module detection (Power JD et al. 2011). In the present study, all nodes in the networks after thresholding were connected, and the link densities were close to 10% (9.23% and 9.97% for innocuous and noxious condition, respectively). The module detection algorithm is based on maximizing the modularity measurement Q for the network (Newman ME 2006), which is defined as:

$$Q = \frac{1}{l^w} \sum_{i,j \in K} \left(w_{ij} - \frac{k_i^w k_j^w}{l^w} \right) \delta_{m_i, m_j}$$

where l^w is the sum of all weights in the network, w_{ij} is the connection weight between node i and j, k_i^w is the weighted degree of node i, and m_i is the module to which node i belongs ($\delta_{m_i, m_j} = 1$ if $m_i = m_j$, and 0 otherwise).

To examine whether the detected modules were stable across different link density, we varied the thresholds in the range of [$q < 0.01$ (FDR corrected), $q < 0.05$ (FDR corrected), $p < 0.001$, $p < 0.01$, $p < 0.05$]. Module detection algorithm was performed to the thresholded networks with weighted edges (positive only) to estimate the partitions of each condition under different link densities.

Network Properties

Prior to graph theoretic analysis, the connection matrix was thresholded by using a certain threshold. Nodes were considered to be 'neighboring' if their edge survived from thresholding. To characterize the robustness of our analyses, network properties of both weighted and binary networks were calculated and compared. Following the traditional approach (Rubinov M and O Sporns 2010; Power JD *et al*. 2011; Power JD et al. 2013; Xu Y et al. 2016), negative links were excluded from our analysis because the biological meaning of negative functional connectivity remains unclear (Parente F et al. 2018). However, in this case, we did not observe strong negative connectivity (e.g., strength > -0.6). For weighted network, we thresholded the network by preserving only positive links with $p < 0.01$, to remove the near zero links that may represent spurious functional connections (Power JD *et al.* 2010; Rubinov M and O Sporns 2010). For binary network, we performed analyses with varying network sparsity (retaining the strongest 10% to 25% of links in 5% increments), and setting supra-threshold links (edges) to 1 and the rest to 0. This range of sparsity was chosen because it allows for the creation of fully connected graphs that permit a reasonable estimation of the graph metrics during the bootstrap test (see Statistical analysis section). The results are identical whether one includes only positive correlations before binarization or not. In addition, since we focus on task-related responses that are less subject to spurious connectivity from time series artifacts than the more common time series connectivity approach, a higher density threshold is appropriate (e.g., started from 10% density)..

Four common properties of the graph that reflect local and global organization as well as the architecture of the graph, including the clustering coefficient (a measure of graph segregation), characteristic path length (a measure of graph integration), small-world-ness (evaluates the network organization compare to a matched random graph), and modularity (Q, measures the decomposability of a graph into several sparsely interconnected communities), were extracted for both weighted and binary graphs. Though some of them (e.g., clustering coefficient and modularity) may represent some common information, each property contributes unique information to the whole picture of network organization. Notably, for binary graphs, we averaged the graph metrics across link densities to ensure that the differences between conditions were not due to the choice of link density (Lynall M-E et al. 2010; Cohen JR and M D'Esposito 2016; Kaplan CM et al. 2019).

The clustering coefficient of a node is defined as the average intensity of all triangles associated with each node for weighted network, and the number of suprathreshold edges between neighbors of this node divided by all possible edges between its neighbors for binary network. The average cluster coefficient, C, averages this value across nodes. Characteristic path length, L, is the shortest path between pairs of nodes, averaged across all pairs. The higher L value indicates longer route, on average, from node to node, resulting in lower efficiency of information transfer along the graph. The modularity of binary network. These network properties were calculated using the Brain Connectivity Toolbox (Rubinov M and O Sporns 2010).

Typically, a small-world network shows more clustering than a random graph but maintains a similar shortest path length (Watts DJ and SH Strogatz 1998). In other words, a small-world network should meet the following criteria: $\gamma = C_{real}/C_{random} > 1$ and $\lambda = L_{real}/L_{random} \approx 1$, where C_{real} and L_{real} are averaged clustering coefficient and averaged characteristic path length of the real network, respectively; and C_{random} and L_{random} are averaged clustering coefficient and averaged characteristic path length of a matched random network, respectively, generated by preserving the degree of each node but randomizing the nodes' connections 100 times. Small-worldness is defined as $\sigma = \gamma / \lambda$, and a network with $\sigma > 1$ indicates the network is 'small-world'.

Hub region detection

Degree centrality was utilized to measure the nodal importance, which is calculated as the sum of edges connected to a node. Here, nodal degree was calculated based on the weighted thresholded network that only preserved positive links with p values < 0.01. Nodes with Z-scored degree value > 1.5 were defined as hubs of the whole brain. Within-module degree (WD) and participation coefficient (PC) were also calculated as measures related to the role each hub node plays in the network (Guimera R and LAN Amaral 2005; Guimerà R and LAN Amaral 2005). The WD value of node i is defined as

$WD_i = \frac{k_i^m - \overline{k^m}}{\sigma^{k^m}}$, where k_i^m is the weighted degree of node *i* within its own module (*m*), $\overline{k^m}$ is the average of the degree within module *m*, and σ^{k^m} is the SD of degree of nodes in module *m*. The PC value of node *i* is defined as $PC_i = 1 - \sum_{m=1}^{M}\left(\frac{k_i^m}{k_i}\right)^2$, where *M* is the number of modules, and k_i is the total weighted degree of node *i*. Nodes with high WD and low PC values are "provincial" hubs connected to other nodes in the same module (cluster), whereas nodes with low WD but high PC values are "connector" hubs that link different modules together. Here, we defined provincial hubs as those with a z-score z(WD) ≥ 1.5 and z(PC) ≤ 0.3, which primarily connect to nodes within their own modules; and connector hubs as those with z(WD) < 1.5 and z(PC) > 0.6, which predominantly link different modules. Similar definition of provincial hub can also be found in (Cohen JR and M D'Esposito 2016).

Assortativity coefficient, defined as correlation between the strength of nodes (degree) on opposite sides of a connection (E J Newman M 2002), was utilized to investigate whether noxious stimuli influence the assortativity of the network structure. Nodes in an assortative network tend to link with other nodes with similar strength, e.g., hub regions are more strongly clustered with other hub regions, making the network more robust to disruption (E J Newman M 2002; Bassett DS et al. 2008).

Statistical analysis

We performed statistical tests on the difference between noxious and innocuous stimulus on brain activity, functional connectivity and network measures. For brain activity, we performed paired *t*-tests ($p < 0.05$, Bonferroni connected across parcels) on noxious vs. innocuous stimulation. For between-group differences in functional connectivity, Steiger's z test (Steiger JH 1980) for dependent correlations was performed, with FDR correction at $q < 0.05$. For network properties, the bias corrected, accelerated bootstrap tests were performed on painfully hot vs. non-painful warm paired (within-person) differences. This test is preferred because of the expected non-normal distribution of differences in network measures. In each bootstrap iteration, participants were resampled with replacement, and paired noxious vs. innocuous differences in each network property (e.g., C) was calculated. This procedure was repeated 5000 times, and two-tailed, uncorrected p values were calculated from the bootstrap confidence interval. FDR correction with $q < 0.05$ was used for correcting multiple comparisons across connectivity densities.

Contrasting subjectively painful vs. non-painful stimuli

We used Study 2 to investigate how changes in network organization varied according to subjective feelings of pain. In Study 2, participants experienced 6 levels of thermal stimuli and were asked to judge whether each individual stimulus was painful or not (Woo C-W *et al.* 2015). They then rated warmth or pain on separate 100-point VAS scales, coded here as (1-100) or (101-200), respectively. For each participant, we grouped trials rated as non-painful and those rated as painful and averaged these within-condition. These averages were used to identify of networks based on individual differences, and to contrast explicitly painful vs. non-painful conditions.

In addition to the aforementioned analysis, normalized mutual information (NMI) (Kuncheva LI and ST Hadjitodorov 2004; Alexander-Bloch A et al. 2012) was utilized to quantify the similarity of modular partitions between subjective evaluation and objective categorization of pain. NMI is a widely used measure to assess pairwise difference between modular partitions, defined as:

$$NMI(A,B) = \frac{-2\sum_{i=1}^{M_A}\sum_{j=1}^{M_B} N_{ij}\log(\frac{N_{ij}N}{N_i N_j})}{\sum_{i=1}^{M_A} N_i \log(\frac{N_i}{N}) + \sum_{j=1}^{M_B} N_j \log(\frac{N_j}{N})}$$

where A and B are the partitions of two networks; M_A is the number of modules in A; N is the number of nodes in the network; N_i and N_j represent the number of nodes in module i of A and module j of B, respectively; N_{ij} is the number of nodes that the two modules have in common. The NMI lies between 0 and 1, a value close to 1 implies the two partitions are relatively similar.

Results

Regional activity for non-painful warm vs. painfully hot stimuli

The comparison pattern of brain activation differences between innocuous and noxious stimulation is shown in Figure 2. Compared to innocuous stimuli, noxious stimuli significantly activated bilateral insular and opercular cortices, ACC, S2, ventral and caudal inferior frontal gyrus (IFG), medial superior frontal gyrus (SFG), premotor cortex, right anterior superior temporal gyrus (STG), some subcortical tissues (e.g., thalamus), and cerebellum. Significant de-activation induced by painfully hot stimuli was found in the left postcentral gyrus (PoG), ventromedial prefrontal cortex (vmPFC), left middle and inferior temporal gyrus (MTG, ITG), right STG, medial precuneus, and bilateral occipital cortices (paired t-test, Bonferroni corrected, $q < 0.05$). This pattern is consistent with previous findings on evoked pain (Treede R-D et al. 2000; Bushnell M and A Apkarian 2006; Kong J et al. 2010; Mouraux A et al. 2011; Wager TD *et al.* 2013; Favilla S *et al.* 2014; Tanasescu R et al. 2016; Lindquist MA *et al.* 2017).

Altered network properties induced by noxious stimuli

Results from the 5000 paired-sample bootstrap test (see Materials and Methods) showed that noxious (vs. innocuous) stimulation significantly influenced the overall organization of functional networks. We found that increased stimulation intensity caused significant increases in both the brain-wide average shortest path length and clustering coefficient ($p < 0.05$, FDR corrected, see Figure 3A and B), resulting in reduced small-worldness (Figure 3C). This indicates that brain regions are more locally clustered, and less globally connected across local clusters (i.e., reduced global efficiency). These changes are coherent in pointing to more tightly clustered results *within* networks and reduced global connectivity *between* functional networks. We unpack these global changes in more detail below.

Reorganized modular architecture during noxious stimuli

By applying the module detection algorithm, we found significantly lower modularity values (Q) during pain, suggesting pain integrates brain systems into fewer functional communities (i.e., clusters)(Figure 3D). Eight distinct modules were identified in the innocuous condition when preserving only significant positive connections (connections with $q < 0.05$, FDR corrected) in the network, whose spatial distribution is shown in Figure 4A&B (different colors indicate different modules). These modules are consistent with intrinsic functional sub-networks identified in other studies, including networks heuristically termed the cognitive control network (CCN, in red), 'default mode' network (DMN, in orange), sensorimotor network (SMN, in yellow), insular-opercular 'ventral attention' or 'salience' network (ION, in gold), a temporal system (TN, in light green), visual function (VN, in dark green), a subcortical network (SCN, in light blue), and a cerebellum system (CBN, in blue). These system partitions showed high coherence across multiple thresholds (Figure 4C). In addition, CCN, ION and SCN were positively activated under warm stimuli, whereas, some regions of DMN and VN were deactivated (Figure 4D).

By contrast, clustering during noxious stimulation resulted in four modules (Figure E and F), which showed high coherence across multiple thresholds (Figure 4G), and were significantly fewer than during innocuous stimulation (Figure 4I, $p < 0.05$, bootstrap test). Specifically, an integrated 'pain-related super-system' (PS)—so termed because it was the only module of the 4 to be significantly activated for painful events (Figure 4H, Figure S2)—included most of the ION and SCN, and components of the CCN (e.g., anterior cingulate cortex) and SMN. Three other systems (OS) were also detected (Figure 4F). OS1 included most of CCN and parts of DMN, and was neither activated nor de-activated during painful vs. innocuous stimulation (Figure 4H). OS2 included most of DMN and several regions of TN, VN, and ION, and was significantly de-activated during pain (Figure 4G, Figure S2). OS3 included most of SMN, VN, and CBN, and was neither activated nor de-activated during painful stimulation.

Analysis of individual differences in reported pain intensity during noxious stimulation also yielded significant relationships across individuals and studies. For analysis across the 5 studies, the average activity with PS was correlated with increased average pain intensity ($r = 0.21$, $p < 0.05$), and OS2 activity was negatively correlated with pain intensity ($r = -0.19$, $p < 0.05$) (see the black line in Figure S3). Together, multiple regression using the average of PS and OS2 to predict pain yielded a multiple correlation of r = 0.39 ($p < 0.0001$). These findings extend earlier work showing correlations between brain activity and perceived pain (Coghill RC et al. 1999; Koyama T et al. 2005; Baliki MN et al. 2009; Wager TD *et al.* 2013; Atlas LY *et al.* 2014). Specifically, these findings extend earlier studies by demonstrating (a) prediction of individual differences by connectivity in a reproducible set of networks, (b) a much larger sample size, and (c) generalizability across multiple studies. No significant correlation was found between the pain ratings and activity in other sub-systems. Interestingly, the alterations in network structure indicate that these communities likely could not be identified in resting-state studies.

Differences in FC with painful heat versus non-painful warmth

Significant connectivity differences between innocuous vs. noxious stimulation ($q <$

0.05, FDR corrected) are shown in Figure 5A. Red and blue connections indicate positive and negative changes during pain, respectively (see also Table S2 for details). During noxious stimulation, connections within the PS became more positive. The increased connectivity integrated several components within the PS, including the CCN (e.g., mPFC, area 44 and 45, and ACC), ION, SMN (e.g., primary sensory cortex), and SCN. Other increased connections were found mainly between lateral SMN and VN within OS3. We also found most of the connections that connected the PS with other systems were decreased, such as connections with hippocampus and temporal cortices.

These altered connectivity patterns further induced decreased shortest path length within each sub-system and increased shortest path length between different sub-systems (Figure S4A), which may result in rises of local communication but reduction in global efficiency. In addition, the increased connectivity within the PS significantly improved its communication efficiency relative to OS2 and OS3 ($p < 0.05$, bootstrap test); the increase in efficiency compared to OS1 was marginally significant ($p = 0.084$, Figure S4B).

Changes in distribution and function of hub regions during noxious stimuli

Distributions of the whole-brain hub regions were also altered during noxious stimuli, partially paralleling reports of hub disruption in chronic pain (Mansour A *et al.* 2016; Mano H *et al.* 2018; Kaplan CM et al. 2019). As we can observe in Figure 5B, during warm stimulation, hubs were distributed broadly across multiple systems (i.e., CCN, ION and SCN), including regions such as medial SFG, ventral middle frontal gyrus (MFG), STG, insula, basal ganglia and other subcortical tissues (colors indicate functional systems in each condition). During painfully hot stimulation, whole-brain hubs were located mainly within PS, including bilateral insular-opercular cortices, medial prefrontal cortex, ACC, and many subcortical (e.g., striatal) regions, and preferred to link with other hubs rather than non-hub nodes (Figure 5C). Similar findings were also reported in fibromyalgia patients with high pain intensity (Kaplan CM et al. 2019), which showed highly interconnected hubs (rich club) within the PS. We also found significant positive correlations ($r_{innocuous} = 0.47$, $r_{noxious} = 0.64$, $ps < 0.001$) between regional activity and nodal degree (*Z*-scored across nodes) in both conditions (Figure 5D).

The connector vs. provincial roles of hub regions was also quite different for innocuous vs. noxious stimulation. Hub regions in the innocuous condition were mostly connectors with high participation coefficients (PCs) but low within-module degrees (WDs), promoting inter-system connectivity between modules. Hub regions during pain were mostly provincial, with low PCs but high WDs, connecting brain regions within the PS (Figure 5E). The number of connector hubs in the noxious condition was significantly lower than in the innocuous condition (bootstrap test, $p < 0.01$), implying reduced information transfer across systems outside the PS during pain. This was consistent with findings of reduced global efficiency and the increased shortest path length between sub-systems. Thus, in sum, pain results in significantly enhanced connections within a ‘supersystem’ including networks associated with affect, attentional allocation to salient events and motivated action selection, cognitive control and/or representation of context and goal relevance, action initiation and valuation (e.g., striatum), and somatosensory perception. Conversely, pain causes reduced connectivity with other systems involved in emotion, semantics, language, visuospatial processing, and long-term memory.

Altered network organization related to subjective pain experience

Analyses grouping trials into subjectively painful and subjectively non-painful conditions, which was possible for one of the studies (N = 30), yielded similar results in many respects. Pain was associated with higher clustering coefficients and increased path length connecting nodes (i.e., reduced global efficiency), and the reduction in small-worldness was marginally significant ($ps < 0.085$, see Figure 6A). However, modularity was significantly higher during painful than non-painful trials (Figure 6A; see below). The modular structure of networks when grouping trials by subjective pain (see Figure 6B) was similar to the structure identified when grouping trials based on objectively noxious stimuli (≥ 46.3℃; see Figure 4F). The assortativity did not show significant change between the two conditions. The similarity in maps of module membership across the brain was highest for the pairs (painful, noxious) and (non-painful, innocuous), and significantly lower for pairs (non-painful, noxious) and (painful, innocuous) ($p < 0.001$, bootstrap test; Figure 6C), suggesting similar reorganization mode induced by noxious stimuli and pain feeling, though discrepancies in module distribution were observed. The discrepancies, we speculated, may result from individual differences in pain threshold; e.g., some of the participants may have experienced pain during low intensity, nominally innocuous stimulation (intensity < 45.3℃). In addition, paralleling analyses grouped by noxious vs. innocuous stimulus intensity, there was a sharp reduction in the number of connector hubs during subjectively painful vs. non-painful trials, as indicated by reduced participation coefficients (PCs) of the top-ranked hubs ($p < 0.01$, bootstrap test, Figure 6D). Thus, our observations of increased clustering and shortest path length, reduced small-worldness, integration of multiple networks into a 'pain-related super-system', and a shift from connector hubs to provincial hubs were all confirmed to be related to subjective pain reports as well as objectively defined noxious stimulation.

More detailed analyses of changes across four levels of reported pain (non-painful [< 100 on the VAS], 100-120, 120-150, and > 150) helped explain the pattern of changes in global network measures we observed when defining conditions based on subjective pain (Figure S5). Clustering coefficient increased and small-worldness decreased monotonically across four levels of reported pain. Minimum path length and modularity were nonmonotonic, highest for intermediate levels of pain and lower for non-painful or very painful trials. This is likely because as pain increases, path length decreases within a 'pain-related super-system' similar to the one we describe above (red in Figure 6B), but increases between modules. Global path length averages over these changes. It is also likely that some aspects of modular organization are driven in part by thermosensory responses in the physiologically noxious (≥ 46.3°C) vs. innocuous (< 45.3°C) range, irrespective of self-reports. Graph measures more strongly related to noxious stimulus intensity (vs. subjective pain) should show smaller changes and/or different results from those based on objective stimulus intensity, as categories defined based on subjective pain mix noxious and innocuous stimuli. Our results show that global path length and modularity indices show the strongest differences, implying that they are relatively more stimulus-related than pain-related, but that other indices track noxious stimulus intensity and subjective pain in a similar fashion. This study was not designed to permit a full dissociation of stimulus-intensity and subjective pain-related effects, as they are very strongly related in healthy individuals. A full characterization of potential differences should be undertaken in specialized studies and patient populations.

Discussion

The original concept of the "pain neuromatrix" (Melzack R 2005) proposed that pain served to integrate neural systems related to somatosensation, affect and emotion, action, viscerosensation, and homeostatic regulation. Though the term was later co-opted as a shorthand for a set of brain regions typically activated by noxious stimulation (Jones A 1998; Peyron R et al. 2000; Bushnell M and A Apkarian 2006; Tracey I and PW Mantyh 2007; Iannetti GD and A Mouraux 2010), its intended spirit is perhaps better characterized in terms of patterns of connectivity across nociceptive and non-nociceptive circuits. The drive to understand pain in terms of functional connections and global network properties has led to the concept of the 'dynamic pain connectome' (Kucyi A and KD Davis 2015, 2017) and a number of recent papers characterize chronic pain in terms of associations with functional connectivity and network properties (Baliki MN *et al*. 2008; Cauda F *et al*. 2009; Napadow V *et al*. 2010; Jensen KB *et al*. 2012; Kong J *et al*. 2013; Baliki MN *et al*. 2014; Ichesco E et al. 2014; Kucyi A and KD Davis 2015; Hemington KS *et al*. 2016; Mansour A *et al*. 2016; Bosma RL et al. 2018; Mano H *et al*.

2018). This paper extends this work by showing reliable patterns of pain-related changes in connectivity across studies. The eight functional systems we identified during innocuous stimulation were broadly consistent with modules reported in resting-state studies (Damoiseaux J et al. 2006; Menon V 2011; Power JD *et al*. 2011), suggesting that innocuous stimuli do not substantially alter the functional architecture observed at rest. However, pain resulted in substantial changes. Network analyses of stimulus-evoked responses based on both objectively noxious stimulus intensity and subjective pain reports revealed a coherent set of changes in network structure (summarize in Table 2), including: (1) reduced small-worldness, increased clustering coefficients, and a shift from 'connector' hubs to 'provincial' hubs, all changes that imply increased integration *within* large-scale functional networks and reduced connectivity across disparate networks; and (2) an integration (increased coherence) of specific networks present at rest and during innocuous stimulation—namely, the 'cognitive control network' (CCN), insular-opercular 'ventral attention' or 'salience' network (ION), 'somatomotor' (SMN), and subcortical (mainly thalamic and striatal) network—into a highly interconnected 'supersystem' (pain-related system, PS) with increased intra-system connectivity and reduced connectivity with other systems.

Co-activation of brain regions (e.g. regions in the 'pain neuromatrix') may result from common latent causes (e.g., variation in nociceptive input). In many cases, observations of stimulus-dependent connectivity may reflect such latent factors; we would argue that this provides a richer characterization of a functional brain system, but does not definitively prove that the underlying architecture is stimulus-dependent. However, if regions are uncorrelated under one stimulus condition (implying that they are not driven by a common latent cause) but correlated under another condition, this provides stronger evidence for stimulus-dependent changes in network communication. We found that this was the case. Regions uncorrelated during non-painful stimulation (and typically at rest as well) became correlated during painful stimulation. Moreover, connectivity changes that originated from activity changes induced by tasks are independent to the interregional 'inherent connectivity' (Duff EP et al. 2018), though some of the 'inherent connectivity' are likely always driven by task-induced activity that is unmodeled or whose timing and duration differs from the timing in the task model (Geuter S et al. 2016). Indeed, the "communication-through-coherence" theory (Fries, 2005) suggests that effective interactions occur when activated neuronal groups undergo coherent excitability fluctuations. However, they are informative in ways that activation magnitude alone is not, as they describe reorganization of the systems that are co-activated in response to painful stimulation. In addition, importantly, co-activation of a set of brain regions does not imply that these regions are all activated to the same degree for a given individual (i.e., that there would be coherent individual differences), or that activation would predict individual differences in behavior (activity in the PS we identified predicted increased pain sensitivity across individuals and studies, and OS2 activity predicted reduced pain sensitivity), as we observed here. Furthermore, the structure of which functional sub-networks are coherently activated in subsets of individuals, and how this relates to pain sensitivity, is largely uncharted territory. Thus, a main contribution of this paper is to show that stimulus-dependent connectivity changes are an important, measurable property of pain-related systems that can provide a more complete description than measuring activity alone – and that connectivity is particularly for characterizing individual differences in pain sensitivity. We are largely agnostic about whether these connectivity changes reflect a common underlying factor such as stronger input to multiple regions or a change in network architecture; however, two facts point to a substantive change in network architecture. First is the fact that during painful stimulation regions outside typical pain-processing regions begin to inter-correlate. Second, many of these regions are not appreciably correlated at rest. These two pieces of evidence argue against a common-factor interpretation. Though our results were not designed to yield identical patterns to those that might be observed based on time series (within-person) functional connectivity, they were designed to identify differences that are maximally related to the processing of painful stimuli and useful for characterizing individual differences.

One broader interpretation of these findings is that the PS 'supersystem' includes the systems required to perceive and respond to bodily threats at both short and long time-scales, from sensation to action initiation to cognitive planning and longer-term action policies. Because the type of pain we studied is immediate, evoked pain, systems related to long-term memory retrieval and broader contextualization of pain relative to the self—e.g., 'default mode' DMN, including medial PFC and hippocampus—are suppressed and disconnected from the sensorimotor-action-planning ‘supersystem’. This interpretation recognizes that pain is a complex process involving many features beyond nociception (e.g., attention and emotion) (Melzack R and PD Wall 1965; Seminowicz D et al. 2004; Moriarty O et al. 2011), and that DMN and hippocampal connectivity may play a different role in relation to chronic pain (e.g., (Baliki MN *et al.* 2008; Jensen KB *et al.* 2012; Loggia ML *et al.* 2013; Kucyi A *et al.* 2014; Vachon-Presseau E et al. 2016; López-Solà M et al. 2017)).

Increased within-module connectivity facilitates the integration and transmission of pain-related information

The increases in connectivity within the PS coupled with reduced inter-module connectivity may serve to prioritize information processing related pain and redirect attention and processing resources towards noxious stimuli. This may facilitate rapid responses to important exogenous stimuli. This idea is consistent with a previous study indicating that cerebral systems may reorganize during pain to enhance the processing efficiency of pain-related information, resulting in shorter times between nociceptive stimulus-evoked cerebral responses and behavioral reactions (Ploner M et al. 2006; Tiemann L et al. 2018).

More broadly, the pain-related integration of systems we observed may be important for integrating multiple cognitive and affective processes essential for overall pain experience and behavior, including encoding of spatial information and stimuli intensity (Greenspan JD et al. 1999; Bornhövd K *et al*. 2002; Bingel U et al. 2003; Bingel U et al.

2004; Arienzo D et al. 2006), pain perception (Blomqvist A et al. 2000; Garcia-Larrea L 2012), transfer sensory information to motor system (Binkofski F et al. 1999; Favilla S *et al*. 2014) and magnitude estimation (Greenspan JD *et al*. 1999; Bornhövd K *et al*. 2002), processing of emotional salience (Rainville P et al. 1997; Johansen JP et al. 2001; Farrell MJ et al. 2005; Zaki J et al. 2012), mobilizing attentional resources towards stimuli (Davis KD *et al*. 1997), and pain-related decision-making (Wiech K et al. 2010; Roy M et al. 2014). The integration we observed spans systems implementing a collection of inter-related processes (Rainville P 2002; Porro CA 2003).

Conversely, the disconnections we observed between systems may relate to the impairments in cognitive performance that are well-known to accompany pain (Crombez G et al. 1996; Eccleston C and G Crombez 1999; Seminowicz D *et al.* 2004; Buhle J and TD Wager 2010; Kucyi A and KD Davis 2015). Kucyi and Davis found that enhanced DMN activity during pain was associated with mind-wandering away from pain and increased ability to maintain cognitive performance during pain (Kucyi A and KD Davis 2015). More direct tests of the relationship between the connectivity patterns we identify here and cognitive performance during pain should be tested in future studies.

Decreased 'bridge' nodes reduce connectivity linking the PS and other subsystems

Provincial hubs are important for within-network communication, whereas connector hubs facilitate information flow between distinct brain networks (van den Heuvel MP and O Sporns 2013). The significant shift from connector hubs during innocuous stimulation to provincial hubs during painful stimulation suggests that pain reduces inter-system communication. Unlike the PS, which was strongly activated during pain, the other three identified subsystems showed deactivation (OS2) or no activation (OS1, OS3). These systems are often thought to be related to descending pain-inhibitory systems (e.g., ventromedial prefrontal cortex (vmPFC), part of the DMN and OS2 here; (Bingel U et al. 2006; Leknes S et al. 2013)), and are often anti-correlated with pain, as we observed here (Kong J *et al*. 2010; Wager TD *et al*. 2013). In addition to roles in descending inhibition, cortical DMN regions (part of OS2) are strongly connected to the hippocampus, forming a system that may be important for *contextualizing* pain, reducing pain experience in healthy participants and safe contexts (Woo C-W et al. 2017), but increasing pain experience when contexts imply threat (Ploghaus A et al. 1999). Thus, disconnection of PS and other systems may imply reduced contextual influences on pain as noxious stimulus intensity increases. This possibility can be directly tested in future studies.

Comparisons between evoked pain and chronic pain improved the understanding of chronic pain beyond nociception

An important question is how our findings on evoked pain relate to network-level changes in various chronic pain conditions. Integrating and comparing findings across studies, methods, and pain conditions is a complex but crucial endeavor as more studies produce network-level descriptions of pain. Comparing evoked and chronic pain can help identify whether brain changes with chronic pain are limited mainly to nociceptive pathways, or extend beyond nociceptive systems to involve novel functional contributions of non-nociceptive central brain circuits (e.g., (Baliki MN et al. 2006; Mansour A *et al*. 2016; Seminowicz DA and M Moayedi 2017; Woo C-W *et al*. 2017)). When pain correlates are limited mainly to nociceptive pathways, it is more likely that changes are secondary to enhanced nociceptive input from the periphery, and peripheral treatments (e.g., surgery) are more likely to be helpful. Conversely, when changes in extra-nociceptive circuits support pain and functional impairment, peripheral pathology and peripheral treatments are less likely to be important. For this reason, it is important to understand which network-level correlates of chronic pain reflect nociceptive vs. extra-nociceptive systems.

Our findings suggest that during evoked pain, nociceptive areas are increasingly integrated with extra-nociceptive areas important for attention, consciousness, memory, and other aspects of cognition and affect. These changes parallel recent findings of similar network-level changes with chronic pain. For example, Kaplan et al. 2019 identified a ‘rich club’ of highly interconnected regions in fibromyalgia (FM) (Kaplan CM et al. 2019) that is similar to the ‘pain supersystem’ we identified here. The strongest increases in global connectivity in FM vs. controls were found in nociceptive target regions (e.g., mid- and anterior insula), and membership of nociceptive regions (e.g., posterior insula, S1) in the ‘rich club’ was found only in patients with the highest clinical pain intensity. Other studies have focused on extra-nociceptive, global network measures associated with chronic pain (e.g., (Mansour A *et al*. 2016; Mano H *et al*. 2018)). Nonetheless, these networks also share some features with evoked pain network topology identified in our study, including increased connectivity in S1 (Mano H et al. 2018), lateral (putatively sensory) thalamus (Mansour A et al. 2016), and posterior insula (Mansour A et al. 2016).

Another common feature of chronic pain is increased connectivity between nociceptive and default-mode regions (Hemington KS *et al*. 2016), paralleling the increased integration between nociceptive and other systems we found in this study. Multiple studies have found pain-related, between-network connectivity increases in DMN-ION (Baliki MN et al. 2014; Kim J et al. 2019), DMN-pain (e.g., (Hashmi JA et al. 2013; López-Solà M *et al*. 2017)) and VN-SMN (Shen W et al. 2019). Thus, some brain network-level changes with chronic pain may be related to the pain itself, either as a predisposing factor or consequence (Baliki MN et al. 2014); others may be truly extra-nociceptive differences in the kinds of patients with chronic pain or correlates of functional, behavioral, and emotional changes beyond pain experience itself. For example, changes in fronto-striatal systems may be associated with withdrawal and avoidance (Roy M *et al*. 2014; Ren W et al. 2016; Schwartz N et al. 2017).

It is interesting when compared with the results of Lee et al. (Lee U et al. 2018), who showed decreased frequency assortativity in chronic pain patients. This difference suggests that there are qualitative differences between brain changes associated with evoked pain and changes in baseline connectivity that develop with chronic pain. Our results suggest that the spread of activity is limited to one system (albeit one that is substantially expanded relative to the resting state) and hubs regions were more inclined to connect with each other, whereas chronic pain patients may experience broader across-module connectivity that makes them vulnerable to explosive synchronization with strong input (Lee U et al. 2018). However, changes in chronic pain are complex, and there are also similarities between our findings and module organization with chronic pain (Kaplan CM et al. 2019), e.g., brain regions within the PS (e.g., insula, ACC and primary somatosensory) are more tensely connected with the increase of clinical pain.

Though the integration of findings across various types of evoked and chronic pain is an important goal, there are also inconsistencies that make integration challenging. These include differences in methods (e.g., hub centrality metrics and region definitions), findings, and emphasis in discussion of what appear inevitably to be complex patterns of effects. For example, thalamic hyperconnectivity is a common feature across disorders in Mansour et al. 2016, but subcortical regions were not tested in some other studies (e.g., Kaplan et al. 2019). Posterior insula changes are a central focus in Kaplan et al. 2019, and some corroborating evidence is apparent in figures in Mansour et al. 2016, but this is not discussed. These incompatibilities could be harmonized in future studies in meta-analyses that directly integrate and compare data across types of stimuli, brain measures, and pain conditions.

Implications for understanding pain consciousness

Another important, seldom addressed question concerns what makes pain conscious. Pain is by definition a subjective, reportable experience, implying consciousness as a required element; but our understanding of what makes pain conscious is limited. Some researchers have described pain as an emergent, global property (Baliki MN and AV Apkarian 2015). While there are multiple theories of consciousness with different brain substrates (Boly M et al. 2012; Bonhomme VLG et al. 2012; Heine L et al. 2012; Barttfeld P et al. 2015; Morsella E et al. 2016; Tononi G et al. 2016), one prominent theory—the "global workspace" theory—posits that integration of activity in the lateral prefrontal cortex amplifies representations in other cortical areas that would otherwise be subliminal, rendering them conscious. Our findings that pain integrates somatosensory activity with frontoparietal systems (the CCN here) similar to those identified by the "global workspace" theory are consistent with this view. The conscious experience of pain may require connectivity between cortical targets of nociceptive afferents (generally located in SMN and ION here) and frontoparietal systems (CCN). We found that all of these systems are integrated during pain. These findings are also broadly consistent with previous work showing loss of consciousness is associated with impeded integration of fronto-parietal system (Schrouff J et al. 2011). Interestingly, findings of decreased modularity when aware of noxious stimuli is also consistent with the view that awareness is associated with reductions in modularity (Godwin D et al. 2015).

Other relationships between functional connectivity and conscious experience are also relevant. For example, we found increased connectivity between thalamus and SMN (both part of PS). Previous studies have associated consciousness with thalamocortical connectivity (Alkire MT and J Miller 2005; Boveroux P et al. 2010), and suggested that decreased thalamocortical connectivity during propofol-induced loss of consciousness might block cortical arousal to external stimuli (Boveroux P *et al*. 2010). Thus, the pattern of integration of cortical and subcortical systems we observed here may be related to what makes pain conscious. This hypothesis needs to be examined further in future studies.

Limitations

A number of limitations could productively be addressed by future work. First, our analyses focused on individual differences, and other types of network-level characterizations based on different types of data are possible. Our focus on stimulation-induced responses minimizes sources of variability unrelated to pain (Geerligs L *et al.* 2015; Finn ES *et al.* 2017), but time series connectivity similarities and differences within and between stimulation periods could paint a complementary picture. In addition, our results reflect average network changes, but characteristics may vary across individuals in ways we have not captured here. Constructing a functional network at the individual-person level is still a challenge for single-trial analysis, and the short duration of each trial and the limited number of trials are limitations. Second, we utilized data from 5 independent datasets with varied thermal intensity and duration of stimulation. This is a strength in one sense, as it promotes generalizability across samples, but it may be less sensitive to individual differences within-study when stimulus and acquisition parameters are tightly controlled. In addition, the findings could be further generalized, e.g., to different types of pain. Third, in this study, we attempted to provide a descriptive label for this ‘supersystem’, “pain-related”, as it is indeed empirically pain-related.

However, caution in interpreting its function is warranted, and validating its profile of sensitivity and specificity is an empirical matter. We make no claims that "pain-related" means that the system measures "pain" to the exclusion of any other process. It is still unclear whether the reorganization of the PS is a pain-specific change or whether it can be evoked by other types of salient, intense, affective states (Liang M et al. 2019). Recently, we identified distinct cerebral representations that are related to pain across multiple types (thermal, mechanical, and visceral) and are not shared with cognitive control and negative emotion tasks (Kragel PA *et al*. 2018). Such analyses require generalization and teste of specificity across multiple studies and task conditions; the generalizability and specificity of the PS to pain could productively be further examined using similar approaches. In addition, we speculated the brain functional reorganization may result from the pain protective function, however, other interpretations are also possible. One possible hypothesis could be that the altered modular organization and hub topology may represent an suboptimal or pathological brain state, similar as in patients with chronic pain (Mansour A *et al*. 2016; Lee U *et al*. 2018; Kaplan CM *et al*. 2019). Currently, it is difficult for us to directly examine other views, but we have indicated increased efficiency and assortativity of the PS, suggesting the reorganized network structure do promote the information exchange. More specific exploration will be performed in the future studies. Finally, current community detection algorithms based on modularity maximization may have degeneracy problem especially for large-scale hierarchical networks (Good BH et al. 2010), and the partitions largely rely on the chosen of resolution parameter that determines the scale of detected communities (He Y et al. 2018). Though our findings of the communities are in good accordance with previous literatures (Bushnell M and A Apkarian 2006; Kong J *et al*. 2010; Power JD *et al*. 2011; Wager TD *et al*. 2013), whether these results are sensitive to the chosen of algorithms and the resolution parameters still need further exploration. This is beyond the scope of the present study, but will be investigated in our future work through varying resolution parameters, and via different modular detection algorithms (e.g., local community methods (Clauset A 2005; Bagrow JP 2008) and generative models (Rosvall M and CT Bergstrom 2007; Clauset A et al. 2008; Hofman JM and CH Wiggins 2008)).

Conclusion

In conclusion, our study showed that painful stimulation drives a reorganization of functional networks. We found that, when experiencing nociceptive stimuli, the brain complexity of modular organization across brain regions is reduced. This may enable the integration of pain processing across functional subsystem, as well as reduce communication (and access to behavioral output systems) with other systems that have less correlation with pain. The subjective pain experience induced similar changes in network organization. These alterations enable a person to rapidly respond to painful stimuli, and may bear on understanding the bases of consciousness, especially in the domain of pain.

Acknowledgement

Funding: This work was supported by NIH grant R01 MH076136 to T. D. W., National Key Basic Research and Development Program of China (2014CB744600, to B. H.), the National Natural Science Foundation of China (61210010, 61632014, to B. H.), the Program of Beijing Municipal Science & Technology Commission grant Z171100000117005 to B. H., and the scholarship of China Scholarship Council (201606180117) to W. Z.. **Author contributions**: W. Z., and T. D. W. drafted the manuscript. W. Z. conducted data analysis. C.-W. W., L. Y. A., M. R., L. S., A. K., and M. J. contributed neuroimaging data. All authors provided feedback and revised the manuscript. **Conflicts of interest**: authors declare there is no conflict of interest in relation to this work.

References

Alexander-Bloch A, Lambiotte R, Roberts B, Giedd J, Gogtay N, Bullmore E. 2012. The discovery of population differences in network community structure: New methods and applications to brain functional networks in schizophrenia. NeuroImage. 59:3889-3900.

Alkire MT, Miller J. 2005. General anesthesia and the neural correlates of consciousness. Progress in brain research. 150:229-597.

Apkarian AV, Bushnell MC, Treede RD, Zubieta JK. 2005. Human brain mechanisms of pain perception and regulation in health and disease. European journal of pain. 9:463-463.

Arienzo D, Babiloni C, Ferretti A, Caulo M, Del Gratta C, Tartaro A, Rossini P, Romani G. 2006. Somatotopy of anterior cingulate cortex (ACC) and supplementary motor area (SMA) for electric stimulation of the median and tibial nerves: an fMRI study. NeuroImage. 33:700-705.

Atlas LY, Bolger N, Lindquist MA, Wager TD. 2010. Brain mediators of predictive cue effects on perceived pain. Journal of Neuroscience. 30:12964-12977.

Atlas LY, Lindquist MA, Bolger N, Wager TD. 2014. Brain mediators of the effects of noxious heat on pain. PAIN®. 155:1632-1648.

Atlas LY, Whittington RA, Lindquist MA, Wielgosz J, Sonty N, Wager TD. 2012. Dissociable influences of opiates and expectations on pain. Journal of Neuroscience. 32:8053-8064.

Bagrow JP. 2008. Evaluating local community methods in networks. Journal of Statistical Mechanics: Theory and Experiment. 2008:P05001.

Baliki MN, Apkarian AV. 2015. Nociception, pain, negative moods, and behavior selection. Neuron. 87:474-491.

Baliki MN, Baria AT, Apkarian AV. 2011. The cortical rhythms of chronic back pain. Journal of Neuroscience. 31:13981-13990.

Baliki MN, Chialvo DR, Geha PY, Levy RM, Harden RN, Parrish TB, Apkarian AV. 2006. Chronic pain and the emotional brain: specific brain activity associated with spontaneous fluctuations of intensity of chronic back pain. J Neurosci. 26:12165-12173.

Baliki MN, Geha PY, Apkarian AV. 2009. Parsing pain perception between nociceptive representation and magnitude estimation. Journal of neurophysiology. 101:875-887.

Baliki MN, Geha PY, Apkarian AV, Chialvo DR. 2008. Beyond feeling: chronic pain hurts the brain, disrupting the default-mode network dynamics. Journal of Neuroscience. 28:1398-1403.

Baliki MN, Mansour AR, Baria AT, Apkarian AV. 2014. Functional reorganization of the default mode network across chronic pain conditions. PloS one. 9:e106133-e106133.

Baliki MN, Mansour AR, Baria AT, Apkarian AV. 2014. Functional reorganization of the default mode network across chronic pain conditions. PloS one. 9:e106133.

Barttfeld P, Uhrig L, Sitt JD, Sigman M, Jarraya B, Dehaene S. 2015. Signature of consciousness in the dynamics of resting-state brain activity. Proceedings of the National

Academy of Sciences. 112:887-892.

Bassett DS, Bullmore E, Verchinski BA, Mattay VS, Weinberger DR, Meyer-Lindenberg A. 2008. Hierarchical organization of human cortical networks in health and schizophrenia. J Neurosci. 28:9239-9248.

Bastuji H, Perchet C, Legrain V, Montes C, Garcia-Larrea L. 2008. Laser evoked responses to painful stimulation persist during sleep and predict subsequent arousals. PAIN®. 137:589-599.

Bingel U, Lorenz J, Glauche V, Knab R, Gläscher J, Weiller C, Büchel C. 2004. Somatotopic organization of human somatosensory cortices for pain: a single trial fMRI study. NeuroImage. 23:224-232.

Bingel U, Lorenz J, Schoell E, Weiller C, Büchel C. 2006. Mechanisms of placebo analgesia: rACC recruitment of a subcortical antinociceptive network. Pain. 120:8-15.

Bingel U, Quante M, Knab R, Bromm B, Weiller C, Büchel C. 2003. Single trial fMRI reveals significant contralateral bias in responses to laser pain within thalamus and somatosensory cortices. NeuroImage. 18:740-748.

Binkofski F, Buccino G, Posse S, Seitz RJ, Rizzolatti G, Freund HJ. 1999. A fronto‐parietal circuit for object manipulation in man: evidence from an fMRI‐study. European Journal of Neuroscience. 11:3276-3286.

Blomqvist A, Zhang E-T, Craig A. 2000. Cytoarchitectonic and immunohistochemical characterization of a specific pain and temperature relay, the posterior portion of the ventral medial nucleus, in the human thalamus. Brain. 123:601-619.

Boly M, Faymonville M-E, Schnakers C, Peigneux P, Lambermont B, Phillips C, Lancellotti P, Luxen A, Lamy M, Moonen G. 2008. Perception of pain in the minimally conscious state with PET activation: an observational study. The Lancet Neurology. 7:1013-1020.

Boly M, Massimini M, Garrido MI, Gosseries O, Noirhomme Q, Laureys S, Soddu A. 2012. Brain connectivity in disorders of consciousness. Brain connectivity. 2:1-10.

Bonhomme VLG, Boveroux P, Brichant JF, Laureys S, Boly M. 2012. Neural correlates of consciousness during general anesthesia using functional magnetic resonance imaging (fMRI). Archives italiennes de biologie. 150:155-163.

Bornhövd K, Quante M, Glauche V, Bromm B, Weiller C, Büchel C. 2002. Painful stimuli evoke different stimulus – response functions in the amygdala, prefrontal, insula and somatosensory cortex: a single - trial fMRI study. Brain. 125:1326-1336.

Bosma RL, Kim JA, Cheng JC, Rogachov A, Hemington KS, Osborne NR, Oh J, Davis KD. 2018. Dynamic pain connectome functional connectivity and oscillations reflect multiple sclerosis pain. Pain. 159:2267-2276.

Boveroux P, Vanhaudenhuyse A, Bruno M-A, Noirhomme Q, Lauwick S, Luxen A, Degueldre C, Plenevaux A, Schnakers C, Phillips C. 2010. Breakdown of within-and between-network resting state functional magnetic resonance imaging connectivity during propofol-induced loss of consciousness. Anesthesiology: The Journal of the American Society of Anesthesiologists. 113:1038-1053.

Buhle J, Wager TD. 2010. Does meditation training lead to enduring changes in the anticipation and experience of pain? Pain. 150:382-383.

Bullmore E, Sporns O. 2009. Complex brain networks: graph theoretical analysis of structural and functional systems. Nature reviews Neuroscience. 10:186.

Bushnell M, Apkarian A. 2006. Representation of pain in the brain. In. Wall and Melzack's Textbook of Pain, 5th edition Elsevier.

Cauda F, Sacco K, Duca S, Cocito D, D'Agata F, Geminiani GC, Canavero S. 2009. Altered resting state in diabetic neuropathic pain. PloS one. 4:e4542.

Chen ZJ, He Y, Rosa-Neto P, Germann J, Evans AC. 2008. Revealing modular architecture of human brain structural networks by using cortical thickness from MRI. Cereb Cortex. 18:2374-2381.

Clauset A. 2005. Finding local community structure in networks. Physical Review E. 72:026132.

Clauset A, Moore C, Newman MEJ. 2008. Hierarchical structure and the prediction of missing links in networks. Nature. 453:98.

Coghill RC, Sang CN, Maisog JM, Iadarola MJ. 1999. Pain intensity processing within the human brain: a bilateral, distributed mechanism. Journal of neurophysiology. 82:1934-1943.

Cohen JR, D'Esposito M. 2016. The Segregation and Integration of Distinct Brain Networks and Their Relationship to Cognition. The Journal of Neuroscience. 36:12083-12094.

Crombez G, Eccleston C, Baeyens F, Eelen P. 1996. The disruptive nature of pain: an experimental investigation. Behaviour research and therapy. 34:911-918.

Damoiseaux J, Rombouts S, Barkhof F, Scheltens P, Stam C, Smith SM, Beckmann C. 2006. Consistent resting-state networks across healthy subjects. Proceedings of the national academy of sciences. 103:13848-13853.

Davis KD, Taylor SJ, Crawley AP, Wood ML, Mikulis DJ. 1997. Functional MRI of pain-and attention-related activations in the human cingulate cortex. Journal of Neurophysiology. 77:3370-3380.

Duff EP, Makin T, Cottaar M, Smith SM, Woolrich MW. 2018. Disambiguating brain functional connectivity. NeuroImage. 173:540-550.

E J Newman M. 2002. Assortative Mixing in Networks.

Eccleston C, Crombez G. 1999. Pain demands attention: A cognitive–affective model of the interruptive function of pain. Psychological bulletin. 125:356.

Evans AC. 2013. Networks of anatomical covariance. NeuroImage. 80:489-504.

Fan L, Li H, Zhuo J, Zhang Y, Wang J, Chen L, Yang Z, Chu C, Xie S, Laird AR. 2016. The human brainnetome atlas: a new brain atlas based on connectional architecture. Cerebral Cortex. 26:3508-3526.

Farmer MA, Baliki MN, Apkarian AV. 2012. A dynamic network perspective of chronic pain. Neuroscience letters. 520:197-203.

Farrell MJ, Laird AR, Egan GF. 2005. Brain activity associated with painfully hot stimuli applied to the upper limb: A meta‐analysis. Human brain mapping. 25:129-139.

Favilla S, Huber A, Pagnoni G, Lui F, Facchin P, Cocchi M, Baraldi P, Porro CA.

2014. Ranking brain areas encoding the perceived level of pain from fMRI data. NeuroImage. 90:153-162.

Finn ES, Scheinost D, Finn DM, Shen X, Papademetris X, Constable RT. 2017. Can brain state be manipulated to emphasize individual differences in functional connectivity? NeuroImage.

Fornito A, Zalesky A, Breakspear M. 2015. The connectomics of brain disorders. Nature Reviews Neuroscience. 16:159.

Garcia-Larrea L. 2012. The posterior insular-opercular region and the search of a primary cortex for pain. Neurophysiologie Clinique/Clinical Neurophysiology. 42:299-313.

Geerligs L, Rubinov M, Henson RN. 2015. State and trait components of functional connectivity: individual differences vary with mental state. Journal of Neuroscience. 35:13949-13961.

Geuter S, Lindquist MA, Wager TD. 2016. Fundamentals of Functional Neuroimaging. In: Berntson GG, Cacioppo JT, Tassinary LG, editors. Handbook of Psychophysiology 4 ed. Cambridge: Cambridge University Press p 41-73.

Godwin D, Barry RL, Marois R. 2015. Breakdown of the brain’s functional network modularity with awareness. Proceedings of the National Academy of Sciences. 112:3799-3804.

Good BH, de Montjoye YA, Clauset A. 2010. Performance of modularity maximization in practical contexts. Physical review E, Statistical, nonlinear, and soft matter physics. 81:046106.

Greenspan JD, Lee RR, Lenz FA. 1999. Pain sensitivity alterations as a function of lesion location in the parasylvian cortex. Pain. 81:273-282.

Guimera R, Amaral LAN. 2005. Functional cartography of complex metabolic networks. nature. 433:895.

Guimerà R, Amaral LAN. 2005. Cartography of complex networks: modules and universal roles. J Stat Mech. 2005:nihpa35573-nihpa35573.

Hashmi JA, Baliki MN, Huang L, Baria AT, Torbey S, Hermann KM, Schnitzer TJ, Apkarian AV. 2013. Shape shifting pain: chronification of back pain shifts brain representation from nociceptive to emotional circuits. Brain. 136:2751-2768.

Hashmi JA, Baria AT, Baliki MN, Huang L, Schnitzer TJ, Apkarian AV. 2012. Brain networks predicting placebo analgesia in a clinical trial for chronic back pain. PAIN®. 153:2393-2402.

He Y, Chen Z, Evans A. 2008. Structural insights into aberrant topological patterns of large-scale cortical networks in Alzheimer's disease. The Journal of neuroscience. 28:4756-4766.

He Y, Chen ZJ, Evans AC. 2007. Small-world anatomical networks in the human brain revealed by cortical thickness from MRI. Cerebral cortex. 17:2407-2419.

He Y, Lim S, Fortunato S, Sporns O, Zhang L, Qiu J, Xie P, Zuo X-N. 2018. Reconfiguration of Cortical Networks in MDD Uncovered by Multiscale Community Detection with fMRI.

Heine L, Soddu A, Gómez F, Vanhaudenhuyse A, Tshibanda L, Thonnard M, Charland-Verville V, Kirsch M, Laureys S, Demertzi A. 2012. Resting state networks and consciousness. Frontiers in psychology. 3:295.

Hemington KS, Wu Q, Kucyi A, Inman RD, Davis KD. 2016. Abnormal cross-network functional connectivity in chronic pain and its association with clinical symptoms. Brain Structure and Function. 221:4203-4219.

Herrera LC, Coan A, Marenco L, Cesar CL, Castellano G. 2017. Impact of gray matter signal regression in resting state and language task functional networks. bioRxiv.094078.

Hofman JM, Wiggins CH. 2008. Bayesian Approach to Network Modularity. Physical Review Letters. 100:258701.

Iannetti GD, Mouraux A. 2010. From the neuromatrix to the pain matrix (and back). Experimental brain research. 205:1-12.

Ichesco E, Schmidt-Wilcke T, Bhavsar R, Clauw DJ, Peltier SJ, Kim J, Napadow V, Hampson JP, Kairys AE, Williams DA. 2014. Altered resting state connectivity of the insular cortex in individuals with fibromyalgia. The Journal of Pain. 15:815-826. e811.

Jensen KB, Loitoile R, Kosek E, Petzke F, Carville S, Fransson P, Marcus H, Williams SC, Choy E, Mainguy Y. 2012. Patients with fibromyalgia display less functional connectivity in the brain’s pain inhibitory network. Molecular pain. 8:32.

Johansen JP, Fields HL, Manning BH. 2001. The affective component of pain in rodents: direct evidence for a contribution of the anterior cingulate cortex. Proceedings of the National Academy of Sciences. 98:8077-8082.

Jones A. 1998. The pain matrix and neuropathic pain. Brain: a journal of neurology. 121:783-784.

Kaplan CM, Schrepf A, Vatansever D, Larkin TE, Mawla I, Ichesco E, Kochlefl L, Harte SE, Clauw DJ, Mashour GA, Harris RE. 2019. Functional and neurochemical disruptions of brain hub topology in chronic pain. Pain. 160:973-983.

Kim J, Mawla I, Kong J, Lee J, Gerber J, Ortiz A, Kim H, Chan ST, Loggia ML, Wasan AD, Edwards RR, Gollub RL, Rosen BR, Napadow V. 2019. Somatotopically specific primary somatosensory connectivity to salience and default mode networks encodes clinical pain. Pain.

Kong J, Jensen K, Loiotile R, Cheetham A, Wey H-Y, Tan Y, Rosen B, Smoller JW, Kaptchuk TJ, Gollub RL. 2013. Functional connectivity of the frontoparietal network predicts cognitive modulation of pain. PAIN®. 154:459-467.

Kong J, Loggia ML, Zyloney C, Tu P, LaViolette P, Gollub RL. 2010. Exploring the brain in pain: activations, deactivations and their relation. Pain. 148:257-267.

Kornelsen J, Sboto-Frankenstein U, McIver T, Gervai P, Wacnik P, Berrington N, Tomanek B. 2013. Default mode network functional connectivity altered in failed back surgery syndrome. The Journal of Pain. 14:483-491.

Koyama T, McHaffie JG, Laurienti PJ, Coghill RC. 2005. The subjective experience of pain: where expectations become reality. Proceedings of the National Academy of Sciences of the United States of America. 102:12950-12955.

Kragel PA, Kano M, Van Oudenhove L, Ly HG, Dupont P, Rubio A, Delon-Martin C, Bonaz BL, Manuck SB, Gianaros PJ. 2018. Generalizable representations of pain, cognitive control, and negative emotion in medial frontal cortex. Nature neuroscience.1.

Krishnan A, Woo C-W, Chang LJ, Ruzic L, Gu X, López-Solà M, Jackson PL, Pujol J, Fan J, Wager TD. 2016. Somatic and vicarious pain are represented by dissociable multivariate brain patterns. Elife. 5:e15166.

Kucyi A, Davis KD. 2015. The dynamic pain connectome. Trends in neurosciences. 38:86-95.

Kucyi A, Davis KD. 2017. The neural code for pain: from single-cell electrophysiology to the dynamic pain connectome. The Neuroscientist. 23:397-414.

Kucyi A, Moayedi M, Weissman-Fogel I, Goldberg MB, Freeman BV, Tenenbaum HC, Davis KD. 2014. Enhanced medial prefrontal-default mode network functional connectivity in chronic pain and its association with pain rumination. Journal of Neuroscience. 34:3969-3975.

Kuncheva LI, Hadjitodorov ST editors. Using diversity in cluster ensembles, 2004 IEEE International Conference on Systems, Man and Cybernetics (IEEE Cat. No.04CH37583); 2004 10-13 Oct. 2004. 1214-1219 vol.1212 p.

Kutch JJ, Labus JS, Harris RE, Martucci KT, Farmer MA, Fenske S, Fling C, Ichesco E, Peltier S, Petre B. 2017. Resting-state functional connectivity predicts longitudinal pain symptom change in urologic chronic pelvic pain syndrome: a MAPP network study. Pain. 158:1069-1082.

Kwan CL, Crawley AP, Mikulis DJ, Davis KD. 2000. An fMRI study of the anterior cingulate cortex and surrounding medial wall activations evoked by noxious cutaneous heat and cold stimuli. Pain. 85:359-374.

LaMotte RH, Campbell JN. 1978. Comparison of responses of warm and nociceptive C-fiber afferents in monkey with human judgments of thermal pain. Journal of neurophysiology. 41:509-528.

Lee U, Kim M, Lee K, Kaplan CM, Clauw DJ, Kim S, Mashour GA, Harris RE. 2018. Functional Brain Network Mechanism of Hypersensitivity in Chronic Pain. Journal., doi: 10.1038/s41598-017-18657-4.

Leknes S, Berna C, Lee MC, Snyder GD, Biele G, Tracey I. 2013. The importance of context: when relative relief renders pain pleasant. PAIN®. 154:402-410.

Liang M, Su Q, Mouraux A, Iannetti GD. 2019. Spatial Patterns of Brain Activity Preferentially Reflecting Transient Pain and Stimulus Intensity. Cereb Cortex. 29:2211-2227.

Lindquist MA, Krishnan A, López-Solà M, Jepma M, Woo C-W, Koban L, Roy M, Atlas LY, Schmidt L, Chang LJ. 2017. Group-regularized individual prediction: theory and application to pain. NeuroImage. 145:274-287.

Lindquist MA, Loh JM, Atlas LY, Wager TD. 2009. Modeling the hemodynamic response function in fMRI: efficiency, bias and mis-modeling. NeuroImage. 45:S187-S198.

Loggia ML, Kim J, Gollub RL, Vangel MG, Kirsch I, Kong J, Wasan AD, Napadow

V. 2013. Default mode network connectivity encodes clinical pain: an arterial spin labeling study. PAIN®. 154:24-33.

López-Solà M, Woo C-W, Pujol J, Deus J, Harrison BJ, Monfort J, Wager TD. 2017. Towards a neurophysiological signature for fibromyalgia. Pain. 158:34.

Mano H, Kotecha G, Leibnitz K, Matsubara T, Nakae A, Shenker N, Shibata M, Voon V, Yoshida W, Lee M. 2018. Classification and characterisation of brain network changes in chronic back pain: A multicenter study. Wellcome open research. 3.

Mano H, Seymour B. 2015. Pain: a distributed brain information network? PLoS biology. 13:e1002037.

Mansour A, Baria AT, Tetreault P, Vachon-Presseau E, Chang P-C, Huang L, Apkarian AV, Baliki MN. 2016. Global disruption of degree rank order: a hallmark of chronic pain. Scientific reports. 6.

Martucci KT, Ng P, Mackey S. 2014. Neuroimaging chronic pain: what have we learned and where are we going? Future neurology. 9:615-626.

Melzack R. 2005. Evolution of the neuromatrix theory of pain. The Prithvi Raj Lecture: presented at the third World Congress of World Institute of Pain, Barcelona 2004. Pain Practice. 5:85-94.

Melzack R, Wall PD. 1965. Pain mechanisms: a new theory. Science. 150:971-979.

Menon V. 2011. Large-scale brain networks and psychopathology: a unifying triple network model. Trends in cognitive sciences. 15:483-506.

Moriarty O, McGuire BE, Finn DP. 2011. The effect of pain on cognitive function: a review of clinical and preclinical research. Progress in neurobiology. 93:385-404.

Morsella E, Godwin CA, Jantz TK, Krieger SC, Gazzaley A. 2016. Homing in on consciousness in the nervous system: An action-based synthesis. Behavioral and Brain Sciences. 39.

Mouraux A, Diukova A, Lee MC, Wise RG, Iannetti GD. 2011. A multisensory investigation of the functional significance of the “pain matrix”. NeuroImage. 54:2237-2249.

Napadow V, LaCount L, Park K, As‐Sanie S, Clauw DJ, Harris RE. 2010. Intrinsic brain connectivity in fibromyalgia is associated with chronic pain intensity. Arthritis & Rheumatology. 62:2545-2555.

Newman ME. 2006. Modularity and community structure in networks. Proceedings of the national academy of sciences. 103:8577-8582.

Palaniyappan L, Park B, Balain V, Dangi R, Liddle P. 2015. Abnormalities in structural covariance of cortical gyrification in schizophrenia. Brain Structure and Function. 220:2059-2071.

Parente F, Frascarelli M, Mirigliani A, Di Fabio F, Biondi M, Colosimo AJBI, Behavior. 2018. Negative functional brain networks. 12:467-476.

Peyron R, Laurent B, Garcia-Larrea L. 2000. Functional imaging of brain responses to pain. A review and meta-analysis (2000). Neurophysiologie Clinique/Clinical Neurophysiology. 30:263-288.

Ploghaus A, Tracey I, Gati JS, Clare S, Menon RS, Matthews PM, Rawlins JNP.

1999. Dissociating pain from its anticipation in the human brain. science. 284:1979-1981.

Ploner M, Gross J, Timmermann L, Schnitzler A. 2006. Pain processing is faster than tactile processing in the human brain. Journal of Neuroscience. 26:10879-10882.

Porro CA. 2003. Functional imaging and pain: behavior, perception, and modulation. The Neuroscientist. 9:354-369.

Power JD, Cohen AL, Nelson SM, Wig GS, Barnes KA, Church JA, Vogel AC, Laumann TO, Miezin FM, Schlaggar BL. 2011. Functional network organization of the human brain. Neuron. 72:665-678.

Power JD, Fair DA, Schlaggar BL, Petersen SE. 2010. The development of human functional brain networks. Neuron. 67:735-748.

Power JD, Schlaggar BL, Lessov-Schlaggar CN, Petersen SEJN. 2013. Evidence for hubs in human functional brain networks. 79:798-813.

Price DD, McHAFFIE JG, Larson MA. 1989. Spatial summation of heat-induced pain: influence of stimulus area and spatial separation of stimuli on perceived pain sensation intensity and unpleasantness. Journal of Neurophysiology. 62:1270-1279.

Rainville P. 2002. Brain mechanisms of pain affect and pain modulation. Current opinion in neurobiology. 12:195-204.

Rainville P, Duncan GH, Price DD, Carrier B, Bushnell MC. 1997. Pain affect encoded in human anterior cingulate but not somatosensory cortex. Science. 277:968-971.

Ren W, Centeno MV, Berger S, Wu Y, Na X, Liu X, Kondapalli J, Apkarian AV, Martina M, Surmeier DJ. 2016. The indirect pathway of the nucleus accumbens shell amplifies neuropathic pain. Nat Neurosci. 19:220-222.

Rosvall M, Bergstrom CT. 2007. An information-theoretic framework for resolving community structure in complex networks. 104:7327-7331.

Roy M, Shohamy D, Daw N, Jepma M, Wimmer GE, Wager TD. 2014. Representation of aversive prediction errors in the human periaqueductal gray. Nature neuroscience. 17:1607-1612.

Rubinov M, Sporns O. 2010. Complex network measures of brain connectivity: uses and interpretations. NeuroImage. 52:1059-1069.

Schrouff J, Perlbarg V, Boly M, Marrelec G, Boveroux P, Vanhaudenhuyse A, Bruno M-A, Laureys S, Phillips C, Pélégrini-Issac M. 2011. Brain functional integration decreases during propofol-induced loss of consciousness. NeuroImage. 57:198-205.

Schwartz N, Miller C, Fields HL. 2017. Cortico-Accumbens Regulation of Approach-Avoidance Behavior Is Modified by Experience and Chronic Pain. Cell Reports. 19:1522-1531.

Seminowicz D, Mikulis D, Davis K. 2004. Cognitive modulation of pain-related brain responses depends on behavioral strategy. Pain. 112:48-58.

Seminowicz DA, Davis KD. 2007. Pain enhances functional connectivity of a brain network evoked by performance of a cognitive task. Journal of neurophysiology. 97:3651-3659.

Seminowicz DA, Moayedi M. 2017. The Dorsolateral Prefrontal Cortex in Acute and

Chronic Pain. The journal of pain : official journal of the American Pain Society. 18:1027-1035.

Sha Z, Xia M, Lin Q, Cao M, Tang Y, Xu K, Song H, Wang Z, Wang F, Fox PT. 2017. Meta-Connectomic Analysis Reveals Commonly Disrupted Functional Architectures in Network Modules and Connectors across Brain Disorders. Cerebral Cortex.1-16.

Shen W, Tu Y, Gollub RL, Ortiz A, Napadow V, Yu S, Wilson G, Park J, Lang C, Jung M, Gerber J, Mawla I, Chan S-T, Wasan AD, Edwards RR, Kaptchuk T, Li S, Rosen B, Kong J. 2019. Visual network alterations in brain functional connectivity in chronic low back pain: A resting state functional connectivity and machine learning study. NeuroImage: Clinical. 22:101775.

Simony E, Honey CJ, Chen J, Lositsky O, Yeshurun Y, Wiesel A, Hasson U. 2016. Dynamic reconfiguration of the default mode network during narrative comprehension. Nature communications. 7:12141.

Sporns O, Zwi JD. 2004. The small world of the cerebral cortex. Neuroinformatics. 2:145-162.

Steiger JH. 1980. Tests for comparing elements of a correlation matrix. Psychological bulletin. 87:245.

Tagliazucchi E, Balenzuela P, Fraiman D, Chialvo DR. 2010. Brain resting state is disrupted in chronic back pain patients. Neuroscience letters. 485:26-31.

Tanasescu R, Cottam WJ, Condon L, Tench CR, Auer DP. 2016. Functional reorganisation in chronic pain and neural correlates of pain sensitisation: a coordinate based meta-analysis of 266 cutaneous pain fMRI studies. Neuroscience & Biobehavioral Reviews. 68:120-133.

Tétreault P, Mansour A, Vachon-Presseau E, Schnitzer TJ, Apkarian AV, Baliki MN. 2016. Brain connectivity predicts placebo response across chronic pain clinical trials. PLoS biology. 14:e1002570.

Tiemann L, Hohn VD, Dinh ST, May ES, Nickel MM, Gross J, Ploner M. 2018. Distinct patterns of brain activity mediate perceptual and motor and autonomic responses to noxious stimuli. Nature communications. 9:4487.

Tononi G, Boly M, Massimini M, Koch C. 2016. Integrated information theory: from consciousness to its physical substrate. Nature Reviews Neuroscience. 17:450.

Tracey I, Mantyh PW. 2007. The cerebral signature for pain perception and its modulation. Neuron. 55:377-391.

Treede R-D, Apkarian AV, Bromm B, Greenspan JD, Lenz FA. 2000. Cortical representation of pain: functional characterization of nociceptive areas near the lateral sulcus. Pain. 87:113-119.

Vachon-Presseau E, Tétreault P, Petre B, Huang L, Berger SE, Torbey S, Baria AT, Mansour AR, Hashmi JA, Griffith JW. 2016. Corticolimbic anatomical characteristics predetermine risk for chronic pain. Brain. 139:1958-1970.

van den Heuvel MP, Sporns O. 2013. Network hubs in the human brain. Trends in cognitive sciences. 17:683-696.

Wager TD, Atlas LY, Lindquist MA, Roy M, Woo C-W, Kross E. 2013. An fMRI-based neurologic signature of physical pain. New England Journal of Medicine. 368:1388-1397.

Wager TD, Scott DJ, Zubieta J-K. 2007. Placebo effects on human μ-opioid activity during pain. Proceedings of the National Academy of Sciences. 104:11056-11061.

Watts DJ, Strogatz SH. 1998. Collective dynamics of'small-world'networks. nature. 393:440.

Wiech K. 2016. Deconstructing the sensation of pain: The influence of cognitive processes on pain perception. Science. 354:584-587.

Wiech K, Lin C-s, Brodersen KH, Bingel U, Ploner M, Tracey I. 2010. Anterior insula integrates information about salience into perceptual decisions about pain. Journal of Neuroscience. 30:16324-16331.

Woo C-W, Roy M, Buhle JT, Wager TD. 2015. Distinct brain systems mediate the effects of nociceptive input and self-regulation on pain. PLoS biology. 13:e1002036.

Woo C-W, Schmidt L, Krishnan A, Jepma M, Roy M, Lindquist MA, Atlas LY, Wager TD. 2017. Quantifying cerebral contributions to pain beyond nociception. Nature communications. 8:14211.

Xu Y, Lin Q, Han Z, He Y, Bi YJN. 2016. Intrinsic functional network architecture of human semantic processing: modules and hubs. 132:542-555.

Yao Z, Hu B, Zheng J, Zheng W, Chen X, Gao X, Xie Y, Fang L, Initiative AsDN. 2015. A FDG-PET study of metabolic networks in apolipoprotein E ε4 Allele carriers. PloS one. 10:e0132300.

Zaki J, Davis JI, Ochsner KN. 2012. Overlapping activity in anterior insula during interoception and emotional experience. NeuroImage. 62:493-499.

Zaki J, Ochsner KN, Hanelin J, Wager TD, Mackey SC. 2007. Different circuits for different pain: patterns of functional connectivity reveal distinct networks for processing pain in self and others. Social neuroscience. 2:276-291.

Zheng W, Yao Z, Xie Y, Fan J, Hu B. 2018. Identification of Alzheimer's Disease and Mild Cognitive Impairment Using Networks Constructed Based on Multiple Morphological Brain Features. Biological psychiatry Cognitive neuroscience and neuroimaging. 3:887-897.

Zunhammer M, Bingel U, Wager TD. 2018. Placebo effects on the neurologic pain signature: a meta-analysis of individual participant functional magnetic resonance imaging data. JAMA neurology.

Tables

Table 1. Demographics and study information

Study	Study name	Sample (included)	Sex	Mean age	Duration (s)	Mean temperature by intensity level (°C)	Trial number	Rating scale
Study 1	NSF (Atlas LY *et al.* 2014)	26 (23)	9F	27.8	10	40.8, 43.5, 45.1, 47.0	35 - 48	0 – 10 VAS
Study 2	BMRK3 (Woo C-W *et al.* 2015)	33 (33)	22F	27.9	12.5	44.3, 45.3, 46.3, 47.3, 48.3, 49.3	97	0 – 100 VAS for no-pain and pain, respectively
Study 3	EXP (Atlas LY *et al.* 2010)	17 (15)	9F	25.5	10	41.2, 44.4, 47.2	61 - 64	0 – 10 VAS
Study 4	ILCP (Lindquist MA *et al.* 2017)	29 (24)	16F	20.4	10	44.7, 46.7	64	0 – 100 VAS
Study 5	REMI (Atlas LY *et al.* 2012)	14 (11)	7F	22	11	41.2, 47.1	75	0 – 8 VAS

VAS = visual analog scale

Table 2. Summary of the results

Network metrics		Noxious vs. Innocuous	Painful vs. Non-painful	Interpretation
Shortest path length		↑	↑	· Noxious stimulation results in fewer networks with more efficient intra-network connectivity and greater resistance to disruption. Connectivity between networks is reduced. High pain experience was associated with similar changes. Modularity differences between analyses may reflect competing changes in within- and between-network connectivity (see below).
Clustering coefficient		↑	↑	
Small world-ness		↓	↓ (~)	
Modularity		↓	↑	
Assortativity		↑	*ns*	
Modules		· Innocuous condition: 8 subsystems. · Noxious condition: 4 subsystems. · Components of the ION, SCN, CCN and SMN were reorganized to form the PS.	· Non-painful condition: 6 subsystems (NMI(non-painful & innocuous) = 0.4287). · Painful condition: 4 subsystems (NMI(painful & noxious) = 0.4283).	· There are fewer modules (networks) during painful stimulation and high-pain experience.
Hub regions	Whole brain	· Concentrated within the PS in noxious condition. · Distributed broadly across multiple systems in innocuous condition.		· Brain regions within the PS become more densely connected during painful stimulation.
	Provincial	↑	↑	· Increased intra-module communication.
	Connector	↓	↓	· Decreased inter-module communication.
Connections	Within PS	↑	*ns*	· Increased information transfer within the PS.
	Between systems	↓ (between PS and other systems)		· Disrupted communication between the PS and other systems.

Note: PS = pain-related system; ION = insular-opercular 'ventral attention' or 'salience' network; CCN = cognitive control network; SCN = subcortical network; SMN = sensorimotor network; VN = visual network; NMI = normalized mutual information; *ns* = non-significant; '~' indicates the alteration is marginally significant.

Figures

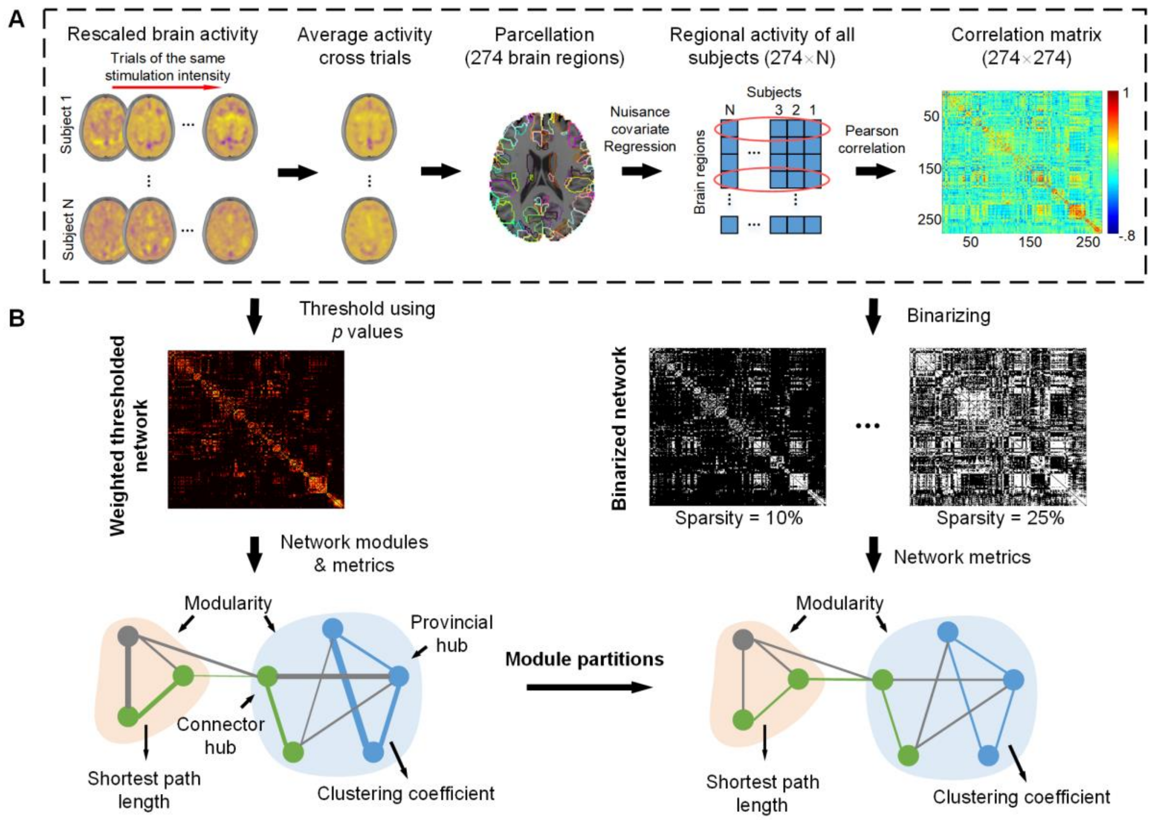

Figure 1. Pipeline of network construction and analysis. (**A**) For each study, pain-related brain activity maps for each trial (from single-trial regression) were rescaled by dividing by the median absolute deviation (MAD) across the entire study, avoiding artifacts related to differences in field strength and other analysis choices that impact the scale of activation maps. The rescaled images were then averaged across trials delivered at the same stimulation intensity within each subject, yielding an average map for each person for each of high- and low-pain intensity. Then, a brain template including 274 brain regions was used to extract the average in-region activity from each trial-averaged image, yielding an N-participants (N = 106) × 274 matrix of pain-related activity values. The global averages of gray matter (GM), white matter (WM) and cerebro-spinal fluid (CSF)

signals were regressed out from the regional activity separately for each study. The functional connectivity between pairs of brain regions was then calculated by measuring the Pearson correlations across individuals, separately for high-pain and low-pain conditions. (**B**) The optimal module partitions were found based on a weighted network by clustering nodes that are densely connected, using correlation values as weights after retaining only edges with significant positive connectivity ($q < 0.05$, FDR corrected). These were then applied to both weighted and binary networks to investigate the differences in network-level graph metrics at multiple levels of network sparsity.

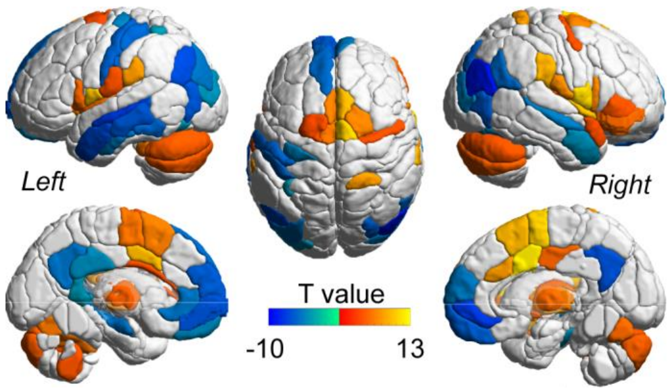

Figure 2. Parcellation of the brain and significant activation (yellow/orange) and deactivation (blue) for noxious vs. innocuous stimulation. Red and blue colors indicate the significance of activity (paired t-test $p < 0.05$, Bonferroni corrected).

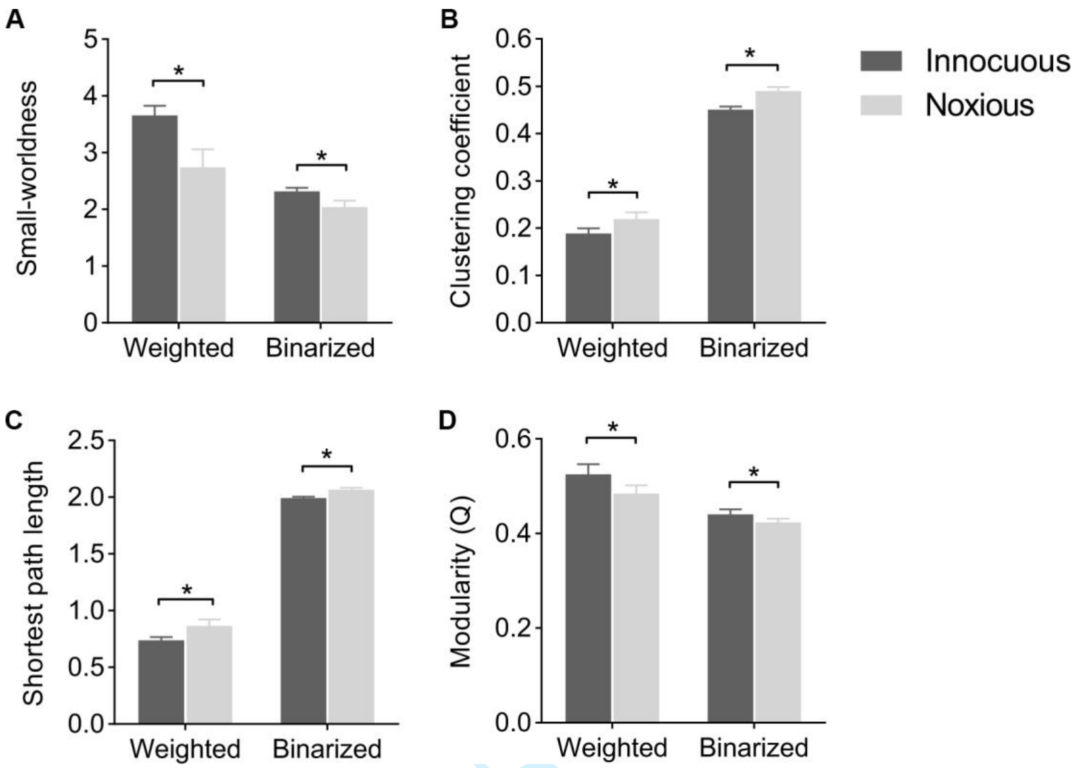

Figure 3. Comparison of network properties between innocuous and noxious stimulations. The network metrics of both weighted and binary networks were extracted. Metrics of weighted network were extracted from networks that only preserved positive links with $p < 0.01$, whereas metrics of binary networks are the average of the graph metrics across link densities (from 10% to 25% in 5% increments). Bars show the mean value and standard deviation from the bootstrap procedure. (**A**) Both networks show small-worldness, but the small-world architecture is disrupted during pain. (**B - D**) Increased average clustering coefficient (*C*) and average characteristic path length (*L*), and deceased modularity (Q) under noxious heat stimulus. Asterisk indicates the p-value exceeds the threshold (bootstrap test, $p < 0.05$).

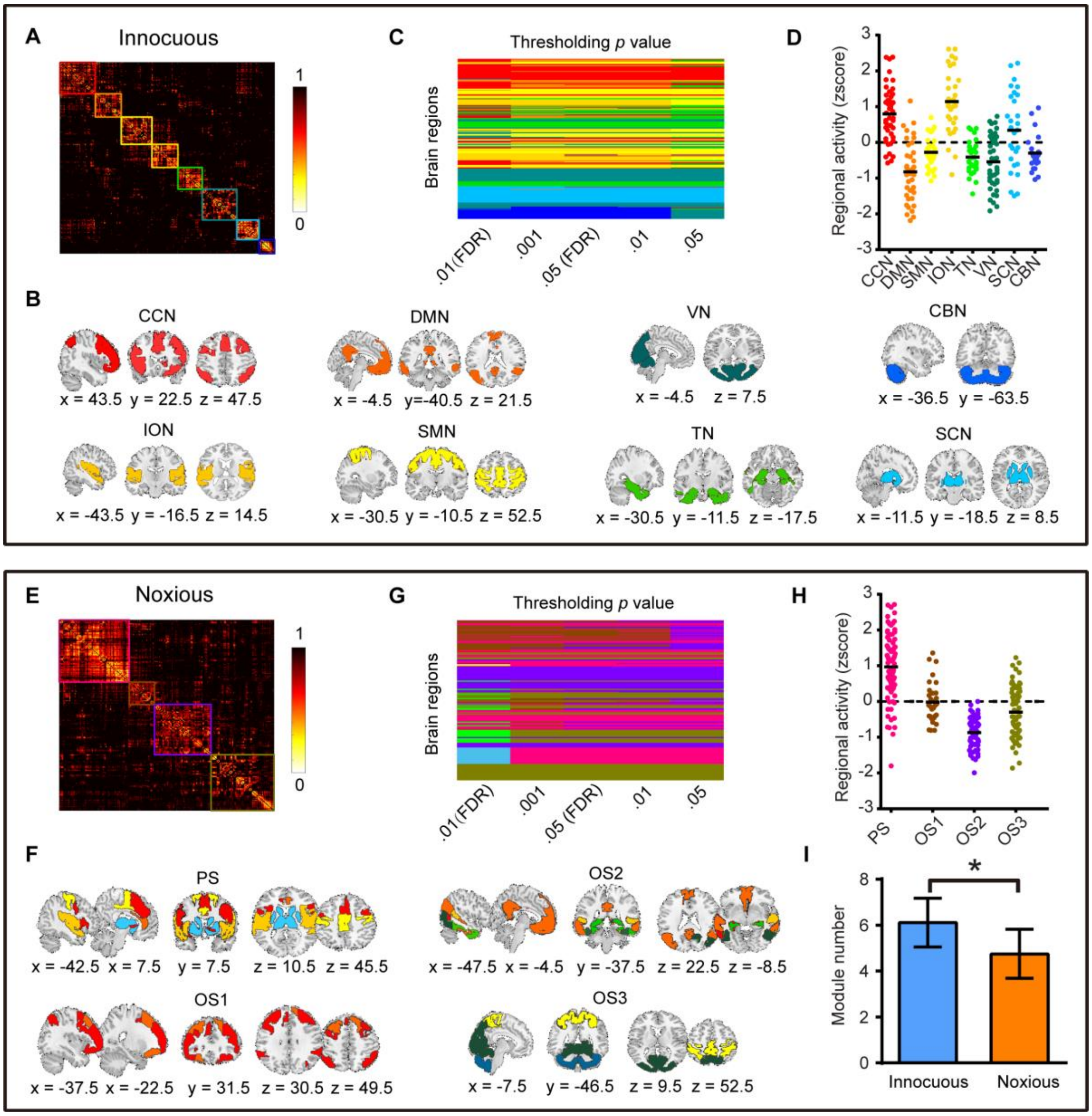

Figure 4. The detected functional systems of each condition. (**A - B**) Visualization of eight functional systems that were detected using network with significant positive connections ($p < 0.05$, FDR corrected) under innocuous stimuli. CCN: cognitive control network; DMN, default mode network; SMN, sensorimotor network; ION, insula-opercular network; TN, temporal network; VN, visual network; SCN, subcortical network; CBN, cerebellum network. (**C**) The coherence modular structure under

innocuous stimuli thresholded by using various p values including [$q < 0.01$ (FDR corrected), $q < 0.05$ (FDR corrected), $p < 0.005$, $p < 0.01$, $p < 0.05$]. Brain regions belong to the same functional system across thresholds are shown in the same color. The partitions are coherent across thresholds, but show a tendency to merge as the threshold p value increases. (**D**) Z-scored activities of brain regions within the systems under innocuous stimuli. (**E - F**) Functional systems detected under painfully hot stimuli (PS = pain-related super-system, OS = other functional system). (**G**) The coherence modular structure under noxious stimuli thresholded by using various p values including [$q < 0.01$ (FDR corrected), $q < 0.05$ (FDR corrected), $p < 0.005$, $p < 0.01$, $p < 0.05$]. Brain regions belong to the same functional system across thresholds are shown in the same color. (**H**) Z-scored regional activities of brain regions within the systems of noxious condition. (**I**) Comparison of module numbers of the two conditions (bootstrap test, $p < 0.05$). Bars show the mean value and standard deviation from the bootstrap procedure.

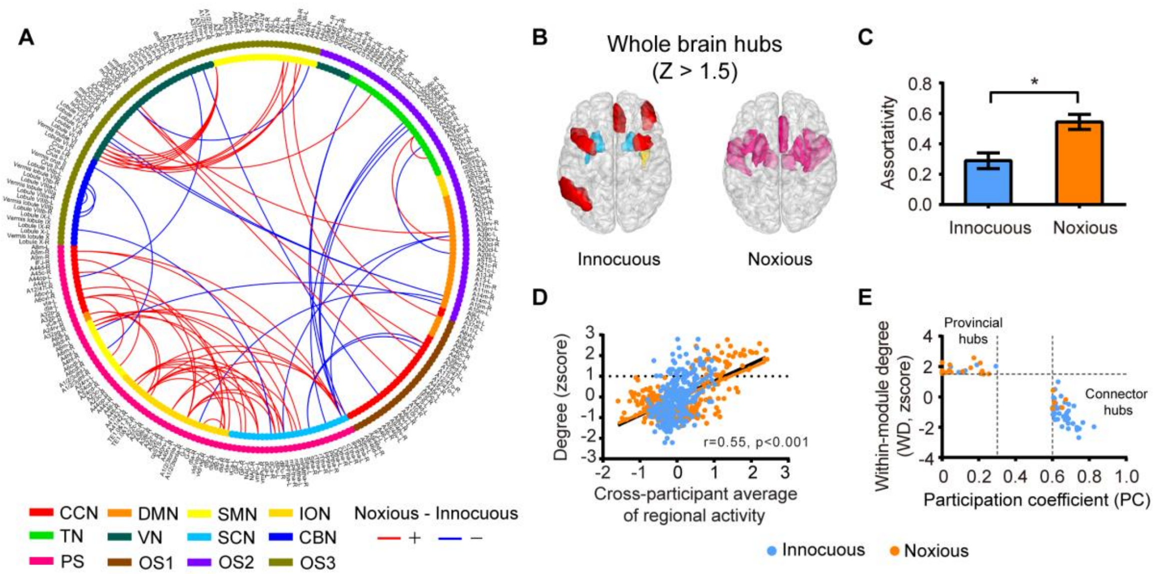

Figure 5. Altered connections and hub regions under noxious stimuli. (**A**) Visualization of the altered connections under noxious stimuli. The lines indicate more positive (red) and negative (blue) connectivity during noxious vs. innocuous stimulation. Colors in the outer ring indicate the functional systems that each brain region belongs to (CCN = cognitive control network; DMN = default mode network; SMN = sensorimotor network; ION = insula-opercular network; TN = temporal network; VN = visual network; SCN = subcortical network; CBN = cerebellum network; PS = pain-related super-system, OS = other functional system). (**B**) Visualization of whole-brain hubs (z-scored degree > 1.5) under non-painful warmth and painfully hot stimulation, respectively. The colors indicate the network membership as in (A) above. During pain, all whole-brain hubs are contained within the PS. (**C**) Differences in assortativity between innocuous and noxious stimuli. Noxious stimulation significantly increases the assortativity of the network ($p < 0.01$). (**D**) The regions with the highest regional activity (averaged across participants) also had

a higher degree on average ($r = 0.55$, $p < 0.001$). Conversely, however, this implies that only 30% of the variance in degree is explained by average activity, and 70% is *not* explained. The correlation under noxious stimuli ($r_{pain} = 0.64$, $p_{pain} < 0.001$) is greater than the correlation in warm condition ($r_{nopain} = 0.47$, $p_{nopain} < 0.001$). (**E**) The distribution of provincial hubs and connector hubs for each condition. The dashed lines indicates the threshold defining provincial hubs (z(WD) = 1.5, z(PC) = 0.3) and connector hub z(WD) = 1.5, z(PC) = 0.6). Provincial hubs are more frequent with painful stimulation, and connector hubs are more frequent with non-painful stimulation.

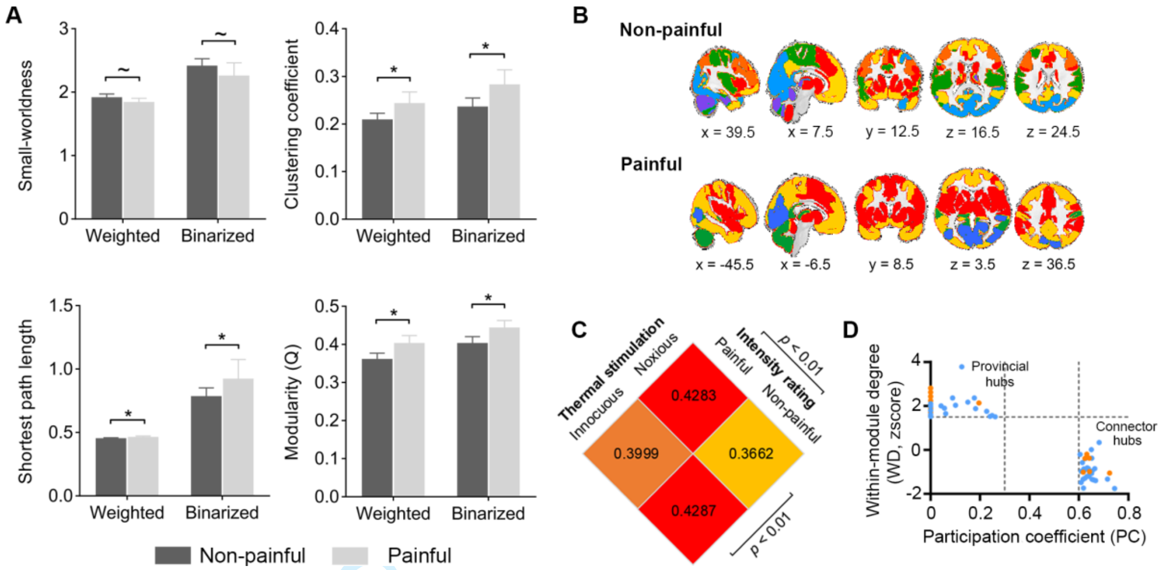

Figure 6. Comparison of network properties, modular organization, and participation coefficient (PC) values of subjective painful vs. non-painful. (**A**) Comparisons of average clustering coefficient (*C*), average characteristic path length (*L*), small-worldness, and modularity (Q) between painful and non-painful conditions. Asterisk indicates the *p* value exceeds the threshold (bootstrap test, $p < 0.05$), '~' indicates the difference is marginally significant. (**B**) Functional subsystems detected in subjective non-painful and painful conditions. (**C**) Comparison of normalized mutual information (NMI) between module segmentations under noxious and innocuous stimuli, and subjective painful and non-painful (bootstrap test, $p < 0.01$). (**D**) The role of hub regions played in each condition. The dashed line indicates the threshold (WD = 1.5, PC = 0.3) between provincial hub and connector hub.

Supplemental Figures

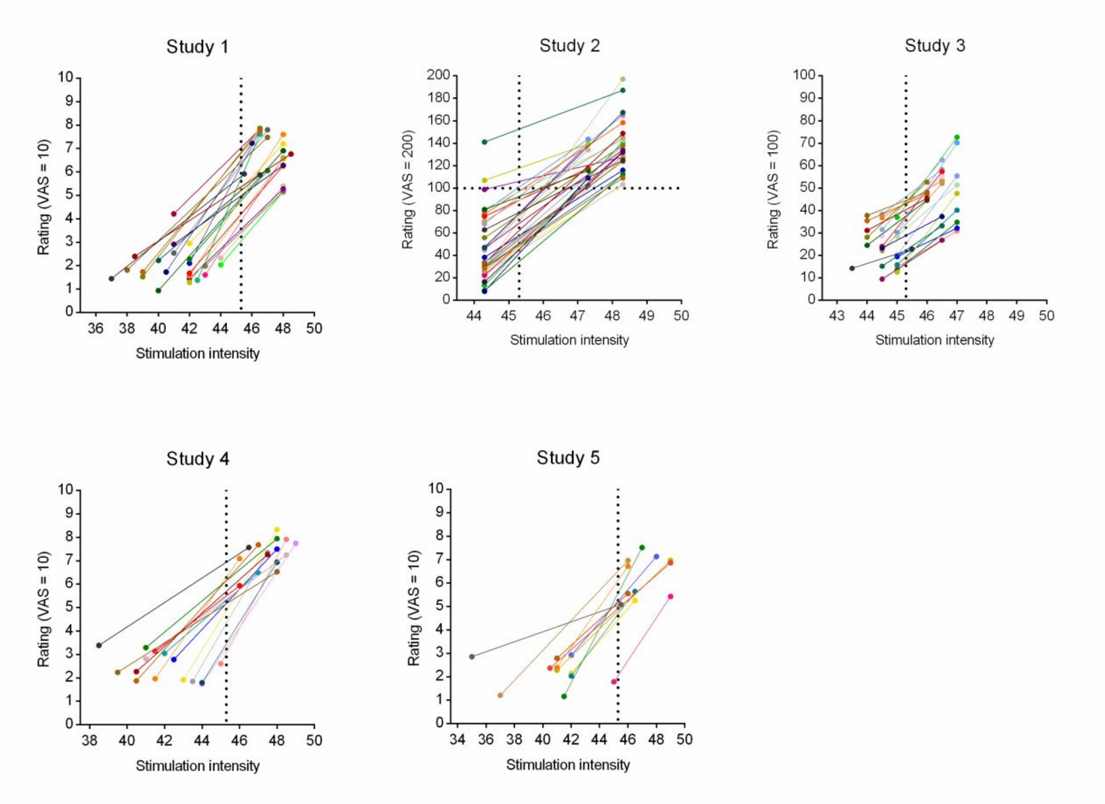

Figure S1. Information of stimulation intensity and pain rating of each dataset (related to Table. 1). Each pair of nodes that connected by a straight line shows the information of one participant. The dashed line indicates the stimulation intensity = 45.3°C.

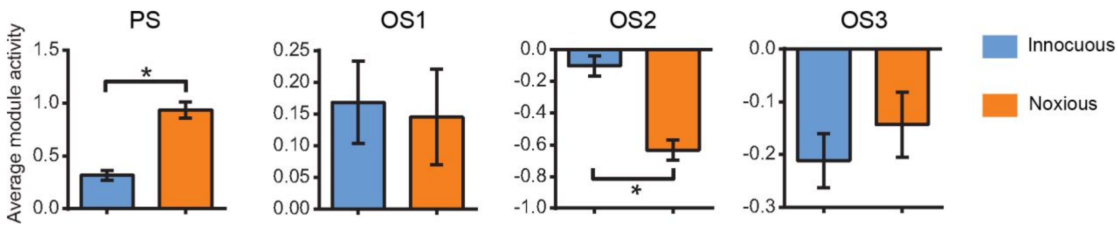

Figure S2. Comparisons of average activities under innocuous warm and noxious stimulations within each pain system (paired t-test, $p < 0.05$). Related to Figure 4. PS, pain-related super-system; OS, other functional system.

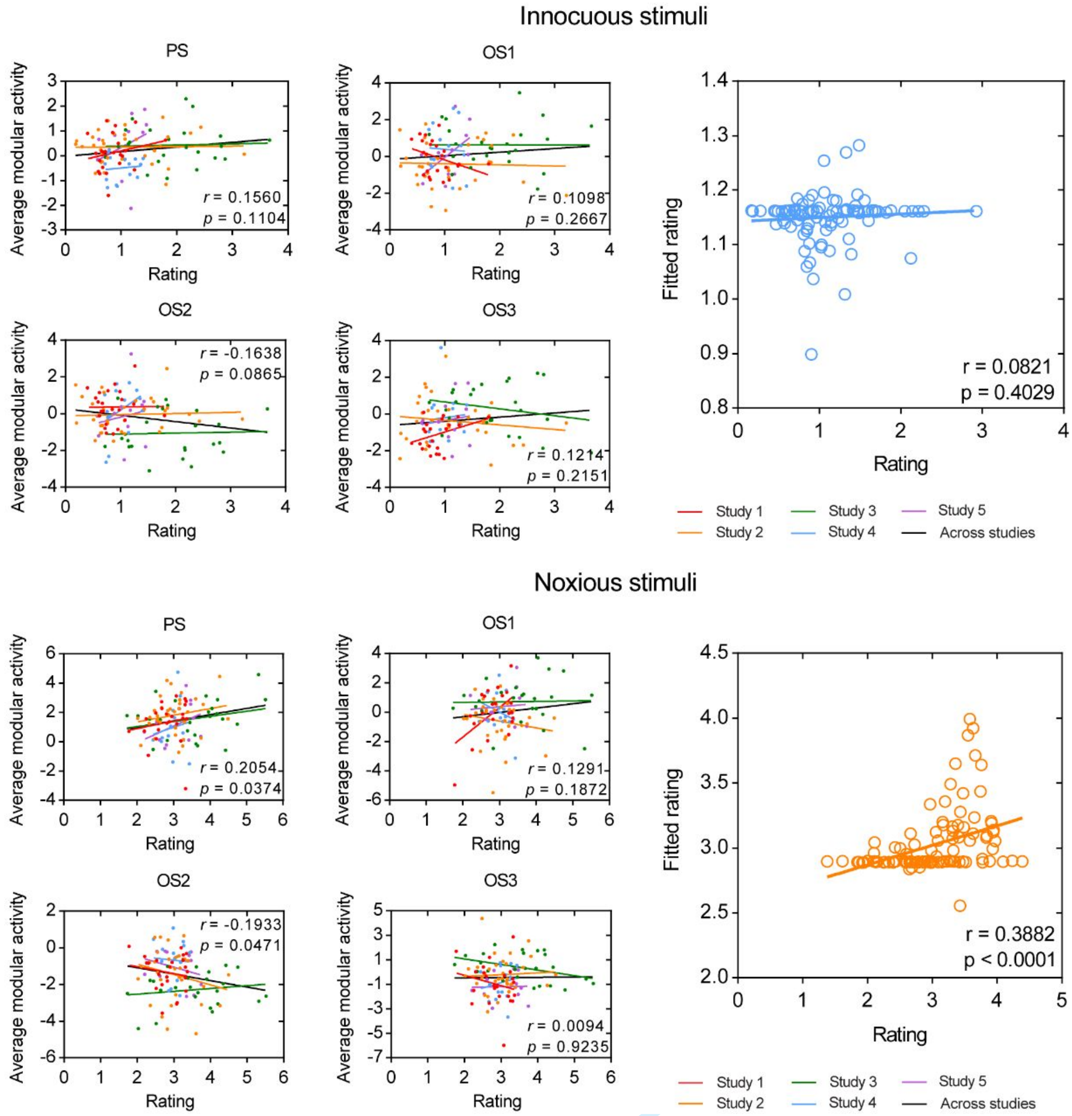

Figure S3. Cross-participant correlations between pain ratings and average activity of each subsystems (related to Figure 4). Instead of the previous preprocessing that regressed nuisance covariates for average GM, WM, and CSF on regional activity, the modular activity here is calculated by first averaging regional activity within a specific module and then regressing the nuisance covariates on the average modular activity. This step was performed for each of the studies separately. To ensure similar scaling of activity across studies, residuals for each study were rescaled by dividing by the median absolute deviation (MAD) of the study. Pearson correlations were then calculated for each of high and low pain conditions to estimate the relationship between individual differences in pain and modular activity. The average activity within PS and OS2 significantly correlated with pain, $r = 0.2054$ ($p = 0.0374$) and $r = -0.1933$ ($p = 0.0471$), respectively, across studies. Colors indicated samples from different cohorts. We further used the average activity values within PS and OS2 as predictors to predict pain rating. The predicted rating significantly correlated rated intensity following noxious stimulation ($r = 0.3882$, $p < 0.0001$), but the correlation was non-significant in the innocuous condition ($p > 0.05$). PS, pain-related super-system; OS, other functional system.

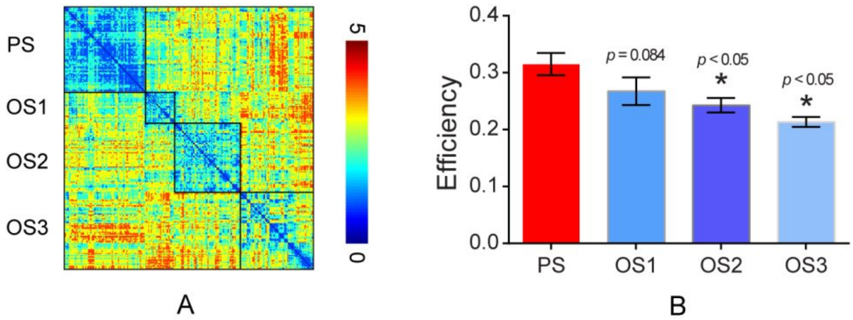

Figure S4. Shortest path length and modular efficiency under noxious heat stimuli (related to Figure 4). (**A**) Graph of shortest path length. Each edge shows the value of shortest path length between the connected two nodes. Black boxes show the sub-systems that detected under painfully hot stimuli (PS = pain-related super-system; OS = other functional system). (**B**) Efficiency of each sub-system. The efficiency of PS is significant higher than the efficiencies of OS2 and OS3 ($p < 0.05$, bootstrap test), and difference between the efficiencies of PS and OS1 is marginally significant ($p = 0.064$).

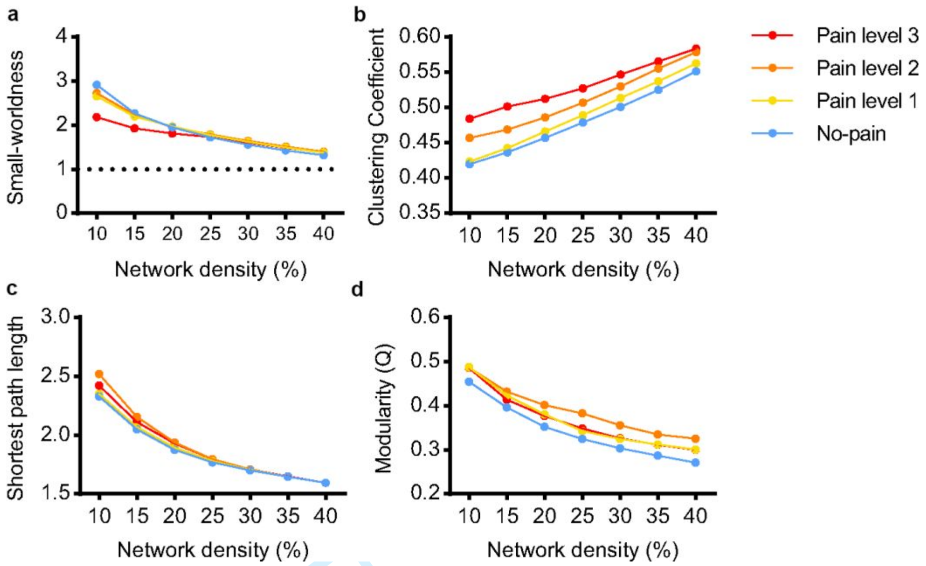

Figure S5. Alterations of network matrices in different level of subjective pain (related to Figure 6). Samples were from Study 2, in which intensity ratings were divided into no-pain (rating < 100), pain level 1 (100 ≤ rating < 120), pain level 2 (120 ≤ rating < 150), and pain level 3 (rating ≥ 150). (**A**) All pain conditions show loss of small-world property, significant difference is only observed between no-pain and pain level 3 at 10% - 15% connective density ($p < 0.05$, bootstrap test, FDR corrected across network density). (**B**) Clustering coefficient grows with the increase of pain. Pain level 2 and pain level 3 show significant higher clustering than no-pain condition ($p < 0.05$, bootstrap test, FDR corrected across network density). (**C**) Higher shortest path length in painful conditions relative to non-painful condition, where the differences between the two highest pain levels and no-pain are significant at 10% connective density ($p < 0.05$, bootstrap test, FDR corrected across network density). (**D**) The modularity of no-pain is significant lower than the three pain conditions ($p < 0.05$, bootstrap test, FDR corrected across network density).

Supplemental Tables

Table S1. Acquisition parameters

Studies	Study locations	Scanners	EPI parameters	Voxel size (mm^3)	Acquisition parameters	Discarded volumes	Stimulus software	Analysis software
Study 1	Columbia	1.5T GE Signa TwinSpeed Excite HD	TR = 2000 ms TE = 34 ms FOV = 224 mm Matrix = 64 × 64	3.5 × 3.5 × 4.0	29 Slices	5	E-prime	SPM8
Study 2	Columbia	3T Phillips Achieva TX	TR = 2000 ms TE = 20 ms FOV = 224 mm Matrix = 64 × 64 Flip angle = 72°	3.0 × 3.0 × 3.0	42 Slices Interleaved SENSE = 1.5	4	E-prime	SPM8
Study 3	Columbia	1.5T GE Signa TwinSpeed Excite HD	TR = 2000 ms TE = 40 ms FOV = 224 mm Matrix = 64 × 64 Flip angle = 84°	3.5 × 3.5 × 4.5	24 Slices $T2^*$-weighted spiral in/out pulse	5	E-prime	SPM5
Study 4	CU Boulder	3T Siemens Tim Trio	TR = 1980 ms TE = 25 ms FOV = 220 mm Matrix = 64×64 Flip angle = 75°	3.4 × 3.4 × 3.0	35 Slices Interleaved iPAT = 2	5	E-prime	SPM8
Study 5	Columbia	1.5T GE Signa TwinSpeed Excite HD	TR = 2000 ms TE = 34 ms FOV = 224 mm Matrix = 64 × 64	3.5 × 3.5 × 4.0	28 Slices	-	E-prime	SPM5

Table S2. Detailed information about the connectivity with significant changes under painful stimuli

Region 1	Region 2	Connectivity strength under painful stimuli	Connectivity strength under non-painful stimuli	Changing Direction	P value
mSFG_R	Stha_L	0.25	-0.26	+	6.60E-05
mSFG_R	lPFtha_L	0.42	-0.11	+	1.60E-05
lSFG_L	mSFG_L	-0.43	0.06	–	8.44E-05
dlSFG_L	dId_R	0.19	-0.32	+	8.65E-05
dlSFG_L	dlPu_R	0.26	-0.28	+	3.13E-05
dlSFG_L	mPMtha_L	0.37	-0.14	+	4.40E-05
dlSFG_R	GP_R	0.44	-0.10	+	1.87E-05
dlSFG_R	lPFtha_L	0.32	-0.17	+	7.29E-05
mSFG_L	gI_R	-0.51	0.06	–	2.72E-06
mSFG_R	Cb_I-IV_L	-0.29	0.25	–	4.96E-05
mSFG_R	Cb_I-IV_R	-0.34	0.28	–	2.54E-06
IFG_R	cdCG_R	0.23	-0.29	+	7.12E-05
vlMFG_R	mPPHC_L	-0.48	0.06	–	1.86E-05
IFS_L	mOccG_R	0.01	-0.52	+	1.09E-05
opIFG_L	tonIaPoG_L	0.45	-0.07	+	5.07E-05
vIFG_L	cSPL_R	-0.44	0.22	–	2.28E-07
lOrG_L	llPCL_L	0.18	-0.36	+	5.45E-05
lOrG_R	llPCL_R	0.22	-0.35	+	1.95E-05
cdlPrG_R	Cb_Crus_I_R	-0.37	0.15	–	6.36E-05
ulPrG_R	mOccG_R	-0.12	0.39	–	8.20E-05
tPrG	Cb_V_R	0.32	-0.25	+	1.55E-05
tPrG	Cb_VI_L	0.38	-0.29	+	2.63E-07
tPrG	Cb_VI_Vermis	0.33	-0.25	+	1.17E-05
tlPrG_L	dId_L	0.75	0.32	+	1.40E-06
tlPrG_L	GP_L	0.48	-0.02	+	3.91E-05
tlPrG_L	vmPu_L	0.49	-0.04	+	1.22E-05
tlPrG_L	dlPu_L	0.56	0.09	+	2.49E-05
tlPrG_R	lPFtha_L	0.33	-0.18	+	4.55E-05
cvlPrG_R	dIg_R	0.52	0.03	+	5.65E-05

llPCL_L	Cb_VI_L	0.13	-0.46	+	4.58E-06
llPCL_R	Cb_VI_L	0.23	-0.28	+	7.09E-05
TE1.0&1.2_L	dId_L	0.64	0.21	+	5.73E-05
TE1.0&1.2_L	rvCG_R	0.43	-0.08	+	8.61E-05
TE1.0&1.2_L	vmPu_L	0.52	-0.04	+	4.33E-06
TE1.0&1.2_L	dlPu_L	0.56	0.04	+	7.71E-06
TE1.0&1.2_L	mPFtha_L	0.31	-0.22	+	5.04E-05
TE1.0&1.2_L	lPFtha_L	0.39	-0.16	+	1.32E-05
TE1.0&1.2_R	rvCG_R	0.47	-0.05	+	3.85E-05
rSTG_R	mPMtha_R	0.23	-0.27	+	7.83E-05
rSTG_R	lPFtha_R	0.24	-0.30	+	3.40E-05
ivITG_L	cvITG_R	0.41	-0.10	+	9.64E-05
rITG_L	ilITG_L	-0.03	0.50	–	2.45E-05
cvITG_L	cvITG_R	0.52	-0.04	+	3.37E-06
rvFuG_R	lPFtha_L	-0.32	0.23	–	2.37E-05
rPhG_L	Otha_L	-0.37	0.24	–	4.91E-06
rPhG_R	lPFtha_L	-0.29	0.28	–	1.22E-05
cIPL_L	mPFtha_L	-0.43	0.16	–	5.05E-06
cIPL_L	lPFtha_L	-0.44	0.16	–	3.79E-06
rdIPL_L	rTtha_L	-0.09	0.42	–	6.92E-05
rdIPL_R	mOccG_L	0.13	-0.39	+	5.64E-05
rdIPL_R	rTtha_L	-0.29	0.30	–	3.24E-06
rvIPL_L	mOccG_R	0.14	-0.38	+	4.92E-05
ulhfPoG_R	dIa_L	0.27	-0.26	+	6.66E-05
tonIaPoG_L	dIa_L	0.55	0.07	+	4.64E-05
tonIaPoG_L	vmPu_L	0.42	-0.15	+	7.72E-06
tonIaPoG_L	dlPu_L	0.52	0.05	+	5.28E-05
tonIaPoG_L	mPFtha_L	0.26	-0.27	+	3.15E-05
truPoG_R	Cb_V_L	0.49	-0.08	+	4.66E-06
truPoG_R	Cb_V_R	0.33	-0.31	+	9.43E-07
truPoG_R	Cb_VI_L	0.45	-0.21	+	1.60E-07
truPoG_R	Cb_VI_Vermis	0.35	-0.28	+	1.14E-06
truPoG_R	Cb_VI_R	0.17	-0.34	+	6.51E-05

dIa_L	dIg_R	0.63	0.20	+	5.82E-05
dIa_R	dId_L	0.68	0.30	+	7.43E-05
dId_L	dId_R	0.77	0.37	+	3.20E-06
lsOccG_L	mAmyg_R	0.20	-0.33	+	9.00E-05
rHipp_R	lPFtha_L	-0.35	0.24	–	5.39E-06
rHipp_R	lPFtha_R	-0.35	0.17	–	7.10E-05
dCa_R	Cb_IX_R	-0.49	0.00	–	6.97E-05
Cb_VIIb_L	Cb_VIIIb_Vermis	0.33	0.72	–	3.11E-05
Cb_VIIb_Vermis	Cb_VIIIb_R	0.07	0.59	–	8.52E-06
Cb_VIIb_R	Cb_VIIIa_R	0.67	0.88	–	1.66E-05

Related to Figure 5